



This is a repository copy of *Aminosilane functionalised aligned fibre PCL scaffolds for peripheral nerve repair*.

White Rose Research Online URL for this paper:

<https://eprints.whiterose.ac.uk/201414/>

Version: Published Version

Article:

Taylor, C.S. orcid.org/0000-0002-9042-9913, Barnes, J., Koduri, M. orcid.org/0000-0002-3760-8373 et al. (6 more authors) (2023) Aminosilane functionalised aligned fibre PCL scaffolds for peripheral nerve repair. *Macromolecular Bioscience*, 23 (11). e2300226. ISSN 1616-5187

<https://doi.org/10.1002/mabi.202300226>

Reuse

This article is distributed under the terms of the Creative Commons Attribution (CC BY) licence. This licence allows you to distribute, remix, tweak, and build upon the work, even commercially, as long as you credit the authors for the original work. More information and the full terms of the licence here:

<https://creativecommons.org/licenses/>

Takedown

If you consider content in White Rose Research Online to be in breach of UK law, please notify us by emailing eprints@whiterose.ac.uk including the URL of the record and the reason for the withdrawal request.



eprints@whiterose.ac.uk
<https://eprints.whiterose.ac.uk/>

Aminosilane Functionalized Aligned Fiber PCL Scaffolds for Peripheral Nerve Repair

Caroline S. Taylor,* Joseph Barnes, Manohar Prasad Koduri, Shamsal Haq, David A. Gregory, Ipsita Roy, Raechelle A. D'Sa, Judith Curran, and John W. Haycock*

Silane modification is a simple and cost-effective tool to modify existing biomaterials for tissue engineering applications. Aminosilane layer deposition has previously been shown to control NG108-15 neuronal cell and primary Schwann cell adhesion and differentiation by controlling deposition of $-NH_2$ groups at the submicron scale across the entirety of a surface by varying silane chain length. This is the first study to report depositing 11-aminoundecyltriethoxysilane (CL11) onto aligned Polycaprolactone (PCL) scaffolds for peripheral nerve regeneration. Fibers are manufactured via electrospinning and characterized using water contact angle measurements, atomic force microscopy (AFM), and X-ray photoelectron spectroscopy (XPS). Confirmed modified fibers are investigated using in vitro cell culture of NG108-15 neuronal cells and primary Schwann cells to determine cell viability, cell differentiation, and phenotype. CL11-modified fibers significantly support NG108-15 neuronal cell and Schwann cell viability. NG108-15 neuronal cell differentiation maintains Schwann cell phenotype compared to unmodified PCL fiber scaffolds. 3D ex vivo culture of Dorsal root ganglion explants (DRGs) confirms further Schwann cell migration and longer neurite outgrowth from DRG explants cultured on CL11 fiber scaffolds compared to unmodified scaffolds. Thus, a reproducible and cost-effective tool is reported to modify biomaterials with functional amine groups that can significantly improve nerve guidance devices and enhance nerve regeneration.

1. Introduction

Injuries to the peripheral nervous system affect 7 million people globally every year, causing long-term pain and disability.^[1] Even with its limitations, such as donor site morbidity and lack of donor nerve availability, the current treatment for large critical gap injuries (20 mm+) remains autografting.^[2] A favorable alternative treatment to autografting is the use of nerve guidance conduits (NGCs), which demonstrate clinical success treating short-gap injuries (10–20 mm). NGCs are manufactured from natural (collagen and chitosan) and synthetic (polycaprolactone (PCL), polylactic glycolic acid (PLGA), and polyvinyl alcohol (PVA) biomaterials using a number of different manufacturing methods.^[3] However, as simple hollow tubular devices, they lack the cellular components, surface chemistry, and topography associated with autograft use that are crucial for successful nerve regeneration. Therefore, several research strategies are being investigated to improve current nerve guide conduits, such as the incorporation of electrospun fibers to provide guidance to the regenerating

axon, and surface modification to provide surface chemistry and topography to improve cell-biomaterial interactions.^[4]

The incorporation of aligned electrospun fibers into the lumen of NGCs is thought to resemble the extracellular matrix and replace/support the formation of the fibrin cable, which forms after implantation of the nerve guide, to guide Schwann cells across the injury site. Aligned fibers, compared to the use of random fibers, have been shown to promote the upregulation of myelin-specific genes, myelin protein zero (PO), and myelin-associated glycoprotein (MAG).^[5] The use of electrospun fibers in NGCs has been shown to extend and improve nerve regeneration capabilities compared to hollow NGCs in ex vivo and in vivo studies.^[6] However, though the incorporation of fibers in the NGC lumen has been found to increase nerve regeneration distance, the regeneration distances measured are not yet sufficient to treat critical nerve gap injury distances, which are 4 cm in a human.^[7] Fibers manufactured from synthetic materials, such as PCL, are inert and lack chemical/topographical cues. Therefore, to further improve and enable nerve repair using aligned fiber synthetic material scaffolds, polymer fibers can be modified using a variety

C. S. Taylor, D. A. Gregory, I. Roy, J. W. Haycock
Department of Materials Science & Engineering, Kroto Research Institute
Broad Lane

Sheffield S3 7HQ, UK

E-mail: c.s.taylor@sheffield.ac.uk; j.w.haycock@sheffield.ac.uk

J. Barnes, M. Prasad Koduri, R. A. D'Sa, J. Curran

Department of Mechanical, Materials and Aerospace, School of Engineering

University of Liverpool


Harrison Hughes Building, Liverpool L69 3GH, UK

S. Haq

Department of Chemistry

University of Liverpool

Crown Street, Liverpool L69 7ZD, UK

 The ORCID identification number(s) for the author(s) of this article can be found under <https://doi.org/10.1002/mabi.202300226>

© 2023 The Authors. Macromolecular Bioscience published by Wiley-VCH GmbH. This is an open access article under the terms of the Creative Commons Attribution License, which permits use, distribution and reproduction in any medium, provided the original work is properly cited.

DOI: 10.1002/mabi.202300226

of techniques, such as coating and surface modification, to improve cell-biomaterial interactions and provide surface chemical and topographical cues to guide regenerating nerve axons.

Functionalizing biomaterials with amine groups has previously been shown to improve neuronal cell-biomaterial interactions.^[8,9] The addition of amine-functionalized nanodiamond to glass substrates was found to support NG108-15 neuronal cell, primary Schwann cell, and primary neuron adhesion and significantly increase neurite outgrowth length in NG108-15 neuronal cells.^[8] Buttiglione et al. also reported that modifying substrates with plasma modification to form amine groups promoted SH-SY5Y cell adhesion and increased neurite elongation.^[9] Several studies have used silane modification to modify biomaterials for tissue engineering applications.^[10] Silane modification is a simple, cost-effective technique to modify biomaterials with chemical reactive groups, including amines, hydroxyls, and carboxyl groups.^[11] Several studies have optimized silane modification for peripheral nerve repair applications. Li et al. functionalized chitosan porous scaffolds with 3-aminopropyl-triethoxysilane (APTES) to promote Schwann cell adhesion on surfaces.^[12] They observed that using 8% APTES in scaffolds promoted an increase in Schwann cell attachment after 24 h in culture, compared to 2% and 5% APTES and chitosan alone.^[12] Joseph et al. cultured neural stem cell spheres on varying chemical groups of self-assembling monolayers (SAMs).^[13] Substrates modified with APTES (to form NH₂-presenting SAMs) showed a significantly higher surface area of neurosphere contact compared to other chemical group SAMs.^[13]

We previously investigated the effect of silane chain length, of the aminosilane, on neuronal and Schwann cell responses on modified glass substrates. To investigate silane chain length on NG108-15 neuronal cell, primary neuron, and primary Schwann cell responses, changing the silane chain length can influence chemical group deposition, leading to changes in surface topography and influencing cell adhesion.^[14] We previously reported that the addition of 11-aminoundecyltriethoxysilane, a long-chain aminosilane (CL11), to plain glass coverslips better supported NG108-15 and primary Schwann cell adhesion, proliferation, and viability compared to using APTES-modified substrates, commonly used in silane modification literature.^[14] We demonstrated a cost-effective, optimized, and scalable method to functionalize glass substrates with NH₂-presenting groups for peripheral nerve repair, providing substrates with a change in surface wettability, rougher topography, and a lower Young's modulus.^[15]

This study is the first of its kind to modify PCL fiber scaffolds with 11-aminoundecyl-triethoxysilane for nerve tissue regeneration applications. PCL fiber scaffolds, 10 µm in diameter, were manufactured via electrospinning, confirming fiber diameter and alignment via scanning electron microscopy.^[7] Successful 11-aminoundecyltriethoxysilane modification of PCL fibers was confirmed via water contact angle, X-ray photoelectron spectroscopy (XPS), and atomic force spectroscopy (AFM) prior to in vitro cell culture using NG108-15 neuronal cells and primary Schwann cells. This study is also the first of its kind to investigate silane-modified substrates using a novel 3D ex vivo fiber testing model using dorsal root ganglion (DRG) explants.^[6,7,15] We describe a cost-effective and scalable way to functionalize PCL fibers with NH₂-presenting groups for nerve repair applications.

2. Results

2.1. PCL Fiber Manufacture and Characterization

Aligned fibers of PCL, with a diameter of 10 µm, were manufactured via electrospinning using the same conditions as previously described.^[7] Modification of PCL fibers using oxygen plasma and CL11 did not alter fiber morphology or diameter as observed in Figure 1A–C. Scanning electron micrographs were quantified to confirm the correct diameter of 10 µm (Figure 1D) had been achieved and that fibers were highly aligned (Figure 1E). Figure 1D confirms that both oxygen plasma and CL11 modification of the PCL fibers did not alter fiber diameter, as no differences in the morphology or diameter were detected. Fiber alignment was confirmed via determining angular variance between fibers, in which 90% of fibers measured in all groups were in the 0–2° group, with very few fibers present in the 2–4° group and no fibers detected in the other groups, confirming the modifications did not alter fiber alignment.

2.2. Changes in PCL Water Contact Angle Using Aminosilane Modification

The addition of oxygen plasma and the addition of oxygen plasma plus CL11 to PCL significantly lowered the PCL water contact angle, from $98.1 \pm 9.7^\circ$ to $80.1 \pm 17.7^\circ$, and $61.7 \pm 5.3^\circ$, respectively (Figure 2). This indicates that PCL alone is hydrophobic, whereas the addition of the modifications decreases the water contact angle and increases hydrophilicity.

2.3. Confirmation of Aminosilane Modification Using X-Ray Photoelectron Spectroscopy

The addition of oxygen plasma and CL11 modification to PCL fibers was confirmed via X-ray photoelectron spectroscopy (XPS). Figure 3B shows an increase in the oxygen peak compared to Figure 3A, confirming oxygen functionalization of the fibers (from 90×10^5 counts per second to 120×10^5 counts per second). Corresponding quantitative data from Table 1 corroborates this by showing an increase in oxygen from $21.3 \pm 0.1\%$ to $29.5 \pm 1.4\%$ following oxygen plasma treatment. Modification of the fibers with CL11 was confirmed by the appearance of a N1s peak in Figure 3C. Corresponding quantitative data from Table 1 confirmed the successful addition of CL11 to PCL fibers by an increase in the atomic percentage of nitrogen from 0% to $2.4 \pm 0.2\%$, respectively.

2.4. Surface Roughness and Adhesion of Treated and Untreated PCL Scaffolds using Atomic Force Microscopy

AFM surface topography (Figure 4A–C) and 3D rendered micrographs (Figure 4D–F) of PCL, PCL plus oxygen plasma, and PCL plus oxygen plasma plus CL11 modified fibers revealed differences in topography and surface roughness. Micrographs were quantified to calculate the typical root mean square (*R_q*) and average roughness (*R_a*) values to determine the surface roughness

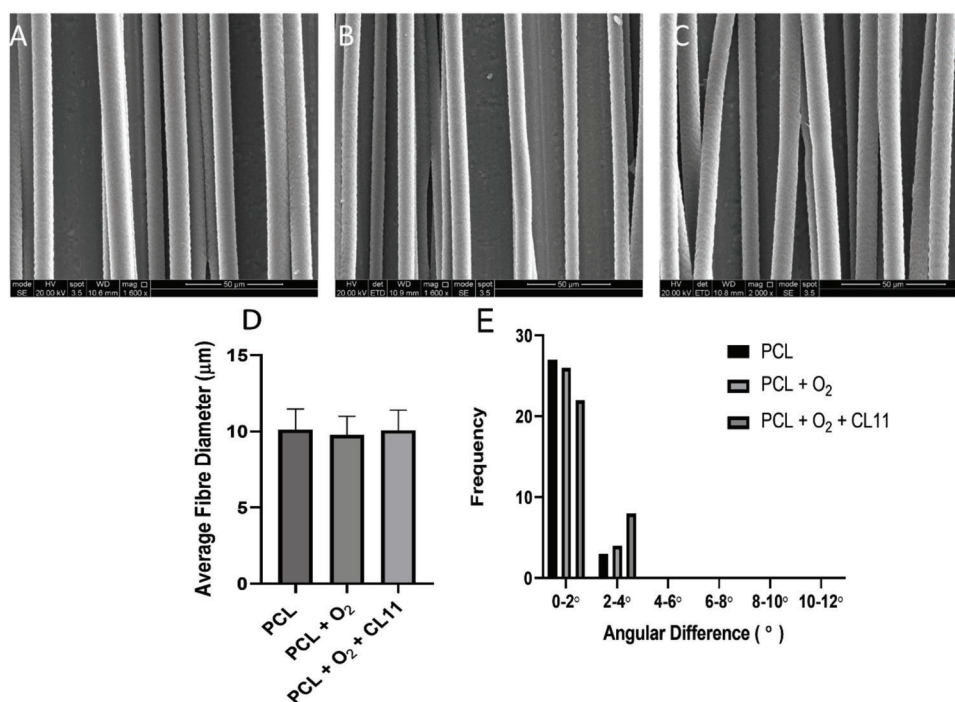


Figure 1. Scanning electron micrographs of A) PCL fibers, B) PCL fibers modified with oxygen plasma, C) PCL fibers modified with oxygen plasma and CL11 (Scale bar = 50 µm). D) Average diameter of polymer fibers. An average of 30 fibers was assessed for each fiber condition and the mean presented (mean \pm SD, $n = 3$ independent experiments). E) Histogram to show the angular variance of fibers. A fiber measured at 180° for each image became a reference line, and the angles of 30 fibers, per condition, measured and placed into categories.

of the fibers, and the values are given in **Table 2**. PCL fibers that had an average R_q value of 55.6 ± 5.3 nm and R_a value of 43.8 ± 1.2 nm. After oxygen plasma treatment (PCL + O₂ fibers), an increase in roughness values was observed with an R_q value of 96.1 ± 6.5 nm and R_a value of 77.3 ± 3.5 nm. The roughness values further increased for the PCL + O₂ + CL11 modified fibers, which exhibited a significantly higher R_q value of 119.0 ± 4.5 nm and R_a value of 94.3 ± 5.4 nm, which is indicative of the silane aggregates forming on the fibers.

AFM adhesion maps (Figure 4G–I) of PCL, PCL plus oxygen plasma, and PCL plus oxygen plasma plus CL11 modified fibers revealed differences in adhesion values. Adhesion is the force measured between the tip of the AFM cantilever, made of silicon nitride, and the fiber sample. The untreated PCL fibers alone revealed to be the most adhesive, measuring 29.1 ± 1.2 nN, whereas after oxygen plasma treatment and oxygen plasma treatment plus CL11, adhesion values recorded were 9.9 ± 0.4 and 11.4 ± 0.9 nN, respectively (values given in Table 2). The addition of CL11 to PCL significantly increased the elastic modulus, from 179.6 ± 11.73 to 215.23 ± 13.34 MPa. No change was observed in the mechanical properties of the PCL when modified with oxygen plasma alone.

2.5. Protein Adsorption on Treated and Untreated PCL Scaffolds

The protein adsorption assay was performed using the Bicinchoninic acid assay to determine the amount of protein adsorbed onto PCL, PCL and oxygen plasma fibers, and PCL and oxygen plasma and CL11 fibers, which was 175 ± 10.08 , 210.35 ± 12.10 ,

and 345.46 ± 11.12 µg cm⁻², respectively (**Figure 5**). Protein adsorption to the PCL fibers significantly increased with the addition of oxygen plasma and CL11 aminosilane to the fibers.

2.6. NG108-15 Neuronal Cell Adhesion and Proliferation on Treated and Untreated PCL Scaffolds

NG108-15 neuronal cell adhesion on the scaffolds was determined using a crystal violet cell adhesion assay. Cell adhesion increased on all scaffolds over the 72 h culture period as seen in **Figure 6A**. No statistical difference was detected in absorbance between the scaffolds after 0.5 h of culture. However, the addition of oxygen plasma and CL11 to the PCL fibers significantly increased the absorbance value at both 24 and 72 h of culture, indicating an increase in cell adhesion. After 72 h, absorbance was significantly higher on the PCL plus oxygen plasma plus CL11 modified fibers compared to PCL alone and oxygen plasma modified PCL fibers, indicating a significant increase in cell adhesion. NG108-15 neuronal cell proliferation activity was measured indirectly using a resazurin assay. Cell proliferation activity, under all conditions, increased over the 168 h time point. At 24, 96, and 168 h in culture, fluorescence values read for the modified PCL fibers (Oxygen plasma and CL11) were significantly higher than unmodified PCL fibers, indicating higher proliferative activity, as seen in **Figure 6B**. Higher proliferative activity of NG108-15 neuronal cells was observed when cells were cultured on PCL fibers modified with only oxygen plasma compared to unmodified PCL

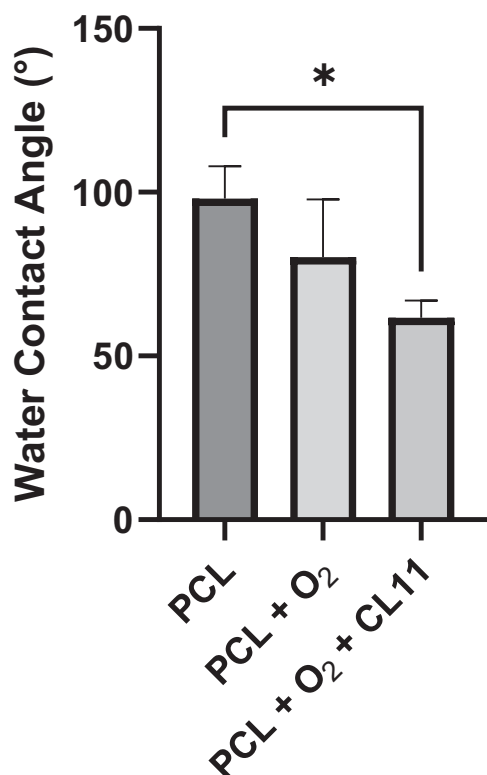


Figure 2. Water contact angle of PCL, PCL fibers modified with oxygen plasma and PCL fibers modified with oxygen plasma and CL11. Results are shown as presented mean (mean \pm SD, $n = 3$ independent experiments; $*p < 0.05$). A total of 9 samples, per condition, were analyzed and a total of 27 contact angles measured per condition.

fibers. However, this effect was only observed at 24 and 168 h time points.

2.7. NG108-15 Neuronal Cell Viability on Treated and Untreated PCL Scaffolds

The effect of modification on NG108-15 neuronal cell viability was investigated using a live/dead assay at 7 days in culture. Confocal micrographs identified that live neuronal cells attached and aligned on all modified and unmodified fibers (Figure 7A–C), and that very few dead cells were observed. After quantification of images, Figure 7D shows that significantly higher numbers of live cells were observed on the CL11 modified fibers (618 ± 46 cells) compared to the oxygen plasma PCL fibers (272 ± 34 cells) and unmodified PCL fibers (159 ± 22 cells). Both modifications significantly increased live NG108-15 neuronal cell attachment. With regard to cell viability, Figure 7E confirms that all substrates supported cell viability of above 98%, and no significant differences were identified between experimental groups.

2.8. NG108-15 Neuronal Cell Differentiation on Treated and Untreated PCL Scaffolds

NG108-15 neuronal cells, cultured on unmodified and modified PCL-aligned fiber scaffolds, were labeled for β III-tubulin and

DAPI (to identify nuclei) to quantify neurite formation. Three fields of view were taken per sample to obtain images: two from the sides and one from the middle of the sample. Outgrowing neurites could be visualized from cells cultured on all fiber scaffolds (Figure 8A–C) but longer neurites could be seen on CL11-modified fiber scaffolds (Figure 8C). Confocal micrographs were quantified to determine average neurite length and the percentage of neurite-bearing cells per substrate as a proxy for nerve regeneration. The average neurite length of neurites measured from NG108-15 neuronal cells cultured on oxygen plasma alone and with CL11 modifications was significantly longer than neurites measured from NG108-15 neuronal cells cultured on unmodified PCL scaffolds (Figure 8D). Average neurite lengths measured were 81.3 ± 14.4 , 137.5 ± 17.4 , and 160.4 ± 27.6 μ m, for PCL fibers, PCL fibers modified with oxygen plasma, and PCL fibers modified with oxygen plasma and CL11, respectively. The percentage of neuronal cells bearing neurites (Figure 8E) for PCL fibers, PCL fibers modified with oxygen plasma, and PCL fibers modified with oxygen plasma and CL11 was $29.8 \pm 13.5\%$, $61.1 \pm 12.4\%$, and $80.6 \pm 21.3\%$, respectively. The percentage of neurite-bearing cells was significantly higher on the modified PCL fibers with CL11 compared to unmodified PCL fibers. No significant differences were detected between oxygen plasma-modified and CL11-modified scaffolds.

2.9. Primary Schwann Cell Adhesion and Proliferation on Treated and Untreated PCL Scaffolds

Rat primary Schwann cell adhesion onto scaffolds was assessed using a crystal violet cell adhesion assay. The addition of the modifications to the PCL fibers did increase initial cell adhesion after 0.5 and 24 h of incubation, as seen in the increase in absorbance values, as seen in Figure 9A. However, this increase was not significant. However, after 72 h in culture, the addition of the modifications to the PCL fibers significantly increased rat primary Schwann cell adhesion. Rat primary Schwann cell proliferation activity was measured indirectly using a resazurin assay at 24, 96, and 168 h time points, presented in Figure 9B. Cell proliferation activity increased significantly on all scaffolds over the 168 h time points, with the greatest effect being observed after 168 h in culture. Both the addition of oxygen plasma alone and the oxygen plasma plus CL11 aminosilane, significantly increased primary Schwann cell proliferation activity, at 24, 96, and 168 h in culture, indicated by the significant increase in fluorescence values.

2.10. Primary Schwann Cell Viability on Treated and Untreated PCL Scaffolds

Modified and unmodified, aligned PCL fibers supported primary Schwann cell attachment and viability, with very few dead cells observed (Figure 10A–C). Schwann cells aligned to fibers in an elongated manner. The CL11 modified PCL fibers supported live Schwann cell attachment significantly better, 269 ± 45 cells, compared to oxygen plasma modified and unmodified PCL fibers, 153 ± 35 cells, and 115 ± 22 cells, respectively (Figure 10D). All fibers, modified and unmodified, supported $>98\%$ cell viability, with no significant differences detected between conditions.

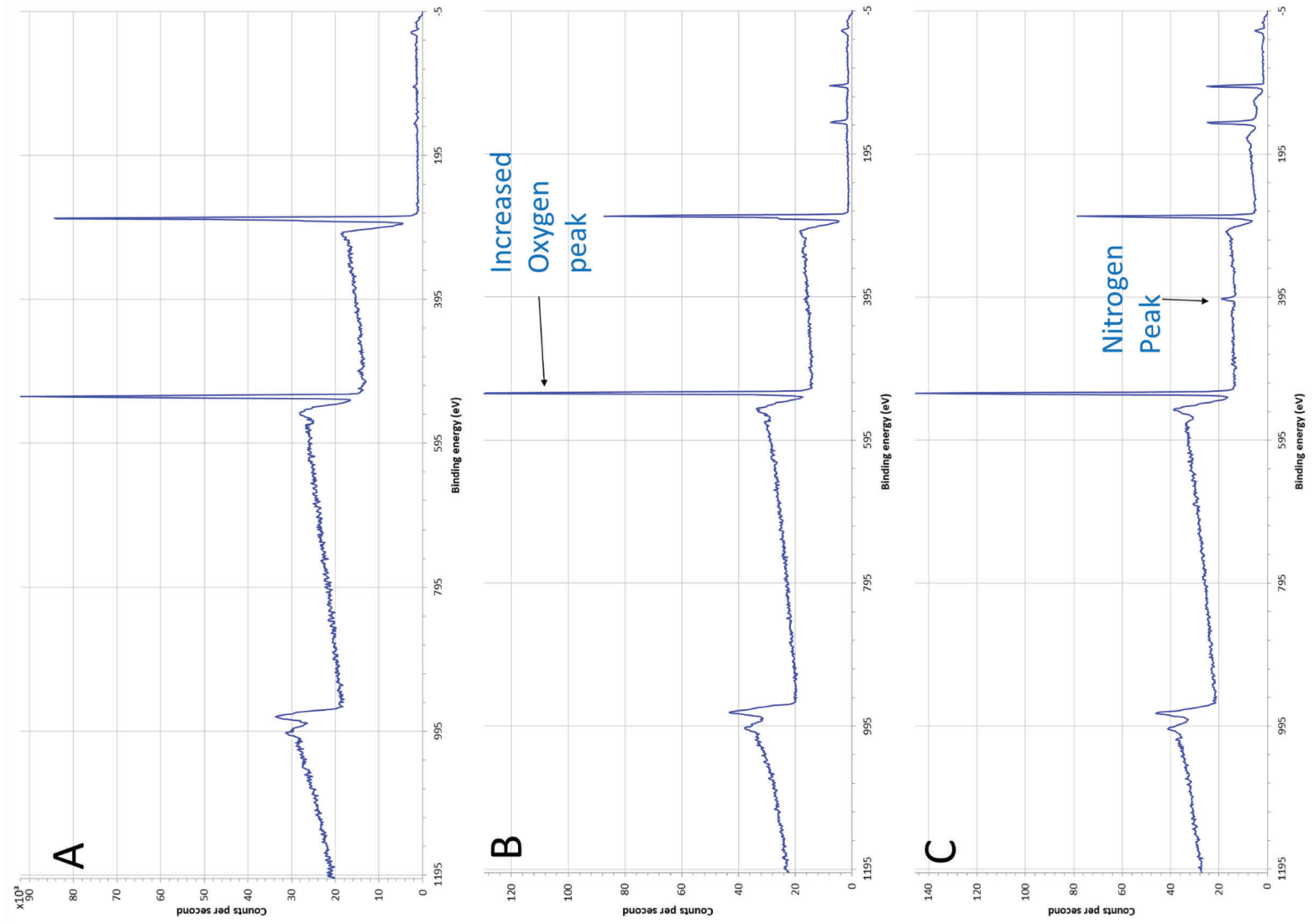


Figure 3. XPS spectra of A) PCL fibers B) PCL + oxygen plasma fibers C) PCL + oxygen plasma fibers (n = 6). A total of 6 spectra per condition were analyzed.

Table 1. XPS characterization of PCL fibers modified with oxygen plasma alone, and oxygen plasma + CL11. XPS elemental composition is shown as percentage of carbon, silicon, oxygen and nitrogen for all modified substrates (data presented as mean \pm SD, $n = 6$).

Sample	At. %			
	C 1s	N 1s	O 1s	Si 2p
PCL	78.7 \pm 0.1	0.0	21.3 \pm 0.1	0.0
PCL + O ₂	61.9 \pm 0.3	0.0	29.5 \pm 1.4	8.6 \pm 3.1
PCL + O ₂ + CL11	54.7 \pm 1.3	2.4 \pm 0.2	30.4 \pm 0.8	12.5 \pm 1.8

2.11. Primary Schwann Cell Phenotype on Treated and Untreated PCL Scaffolds

To confirm that the cell phenotype was maintained, primary Schwann cells cultured on PCL fibers were labeled with S100 β to determine the average Schwann cell length and aspect ratio. Schwann cells adhered to all samples, having an elongated morphology and staining positive for S100 β (Figure 11A–C). No significant differences were detected when calculating the average Schwann cell length of cells cultured on all substrates. The average length of Schwann cells measured on the PCL, oxygen plasma modified PCL, and CL11-modified PCL fibers was 98.7 ± 8.1 , 113.1 ± 8.8 , and 112.1 ± 5.3 μ m, respectively. However, when calculating aspect ratio (length:width), Schwann cells cultured on the PCL fibers had a significantly lower aspect ratio (4.8 ± 1.2 μ m) compared to the aspect ratio of Schwann cells cultured on the CL11 modified fibers (10.1 ± 2.2 μ m). The aspect ratio of Schwann cells cultured on oxygen plasma-modified PCL fibers was 7.2 ± 2.2 μ m.

2.12. Dorsal Root Ganglia Neurite Outgrowth and Schwann Cell Migration on Treated and Untreated PCL Scaffolds

After culture on fibers in a 3D testing system for 7 days, E13 embryonic chick explants were labeled with β III tubulin to assess and measure axon outgrowth and S100 β to identify Schwann cells and measure migration distance from the DRG body. Longer axon outgrowth and Schwann cells observed further from the DRG body could be seen on CL11-modified PCL fibers (Figure 12C) compared to unmodified PCL fibers (Figure 12A) and oxygen plasma-modified fibers (Figure 12B). Axon outgrowth (green) could be seen following migrated Schwann cells (red) and axon outgrowth and Schwann cells were observed co-located, indicating neurite-glial cell contact. Light sheet micrographs were quantified to determine the average axon outgrowth length and Schwann cell migration distance. Average axon outgrowth length (Figure 12D) from DRG explants was significantly longer on CL11-modified fibers (3701.3 ± 321.9 μ m) and oxygen plasma-modified fibers (2862.3 ± 325.6 μ m) compared to unmodified PCL fibers (1262.7 ± 331.5 μ m). Average Schwann cell migration distance (Figure 12D) was significantly higher on CL11-modified fibers (4010.3 ± 312.1 μ m) and oxygen plasma-modified fibers (3234.4 ± 376.4 μ m) compared to unmodified PCL fibers (2237 ± 408.6 μ m).

3. Discussion

Inert biomaterials, such as PCL, have been modified over the years using a variety of techniques to improve cellular adhesion and differentiation by changing the material's surface chemistry and topography.^[16] Silane modification is a cost effective and scalable approach to modifying a biomaterial with a number of different chemical reactive groups.^[11] Our previous work reported on the successful modification of glass substrates using two aminosilanes with varying chain lengths for peripheral nerve repair.^[14] 11-aminoundecyltriethoxysilane, a long-chain aminosilane, was investigated for its potential in nerve repair, compared to 3-aminopropyltriethoxysilane (APTES), a commonly used short-chain aminosilane used to modify biomaterials. We previously reported that 11-aminoundecyltriethoxysilane better supported primary neuron, primary Schwann cell, and NG108-15 neuronal cell adhesion, proliferation, viability, and differentiation compared to APTES-modified substrates due to increasing hydrophilicity and surface roughness and decreasing Young's modulus of the substrates due to chain length.^[14] In this study, we have successfully modified PCL, an FDA-approved polymer used in peripheral nerve repair, with 11-aminoundecyltriethoxysilane for potential use in nerve tissue engineering applications.^[17]

The addition of aligned fibers to the lumen of nerve guidance conduits has been shown to improve nerve regeneration and increase axon outgrowth compared to hollow conduits, though distances are not yet comparable with autograft use.^[6] Aligned fiber scaffolds are currently manufactured with inert materials, resulting in a lack of topography and chemical guidance cues required for successful nerve regeneration. Aligned PCL fiber scaffolds, 10 μ m in diameter, were manufactured by electrospinning using the methods previously described.^[7] Previous studies have shown that the use of aligned fibers, compared to fibers with a random orientation, promotes a mature Schwann cell phenotype,^[5] as seen in vivo, and increases axon outgrowth from DRG explants^[18] as well as regenerating nerves in vivo.^[19] Our previous studies have also shown that aligned fibers in the micrometer range, above 5 μ m, are more effective at promoting neurite outgrowth from neuronal cells and DRGs in vitro.^[7,20]

Modifying PCL with oxygen plasma and CL11 significantly changed PCL fiber surface properties. Lower water contact angles were recorded for oxygen plasma modified and CL11 modified PCL compared to plain PCL alone, indicating the modifications caused the PCL to become less hydrophobic and more hydrophilic in nature (Figure 2). PCL is known to be hydrophobic in nature and have low surface energy values.^[21] The use of oxygen plasma is known to introduce oxygen (polar) functional groups to inert polymers, such as PCL, increasing the surface wettability of the polymer.^[22] Oxygen plasma has been routinely used to increase the surface hydrophilicity and surface wettability of PCL in many different areas of tissue engineering.^[23,24] The addition of amine groups has also been shown to decrease the water contact angle and increase the hydrophilicity of a surface. Sandoval-Castellanos et al. modified tissue culture plastic with amine groups using plasma polymerization of allylamine, which decreased the water contact angle.^[25] Previous work has identified that the addition of 11-aminoundecyltriethoxysilane (CL11) to glass has increased the water contact angle due to the presence of methylene bridges in the aminosilane chain

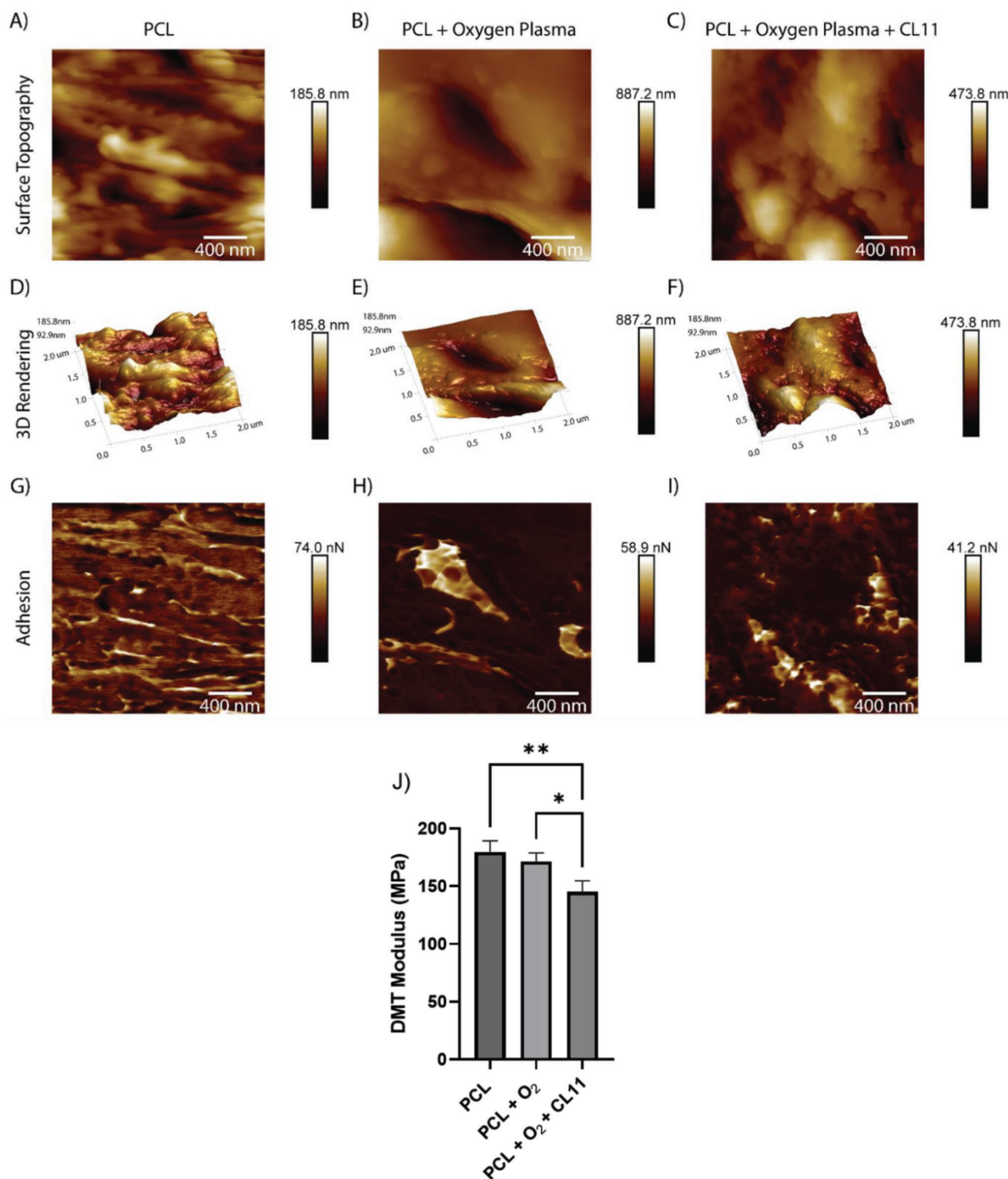


Figure 4. Representative AFM surface topography micrographs of A) PCL fibers, B) PCL + oxygen plasma fibers and C) PCL + oxygen plasma + CL11 fibers, Representative 3D renderings of D) PCL fibers, E) PCL + oxygen plasma fibers and F) PCL + oxygen plasma + CL11 fibers. Representative Adhesion maps of G) PCL fibers, H) PCL + oxygen plasma fibers and I) PCL + oxygen plasma + CL11 fibers. A total of 6 samples, per condition, were imaged. J) Elastic modulus of modified PCL fibers (mean \pm SD, $n = 3$; Three replicates per $n = 1$ and three values taken per sample, * $p < 0.05$ and ** $p < 0.01$).

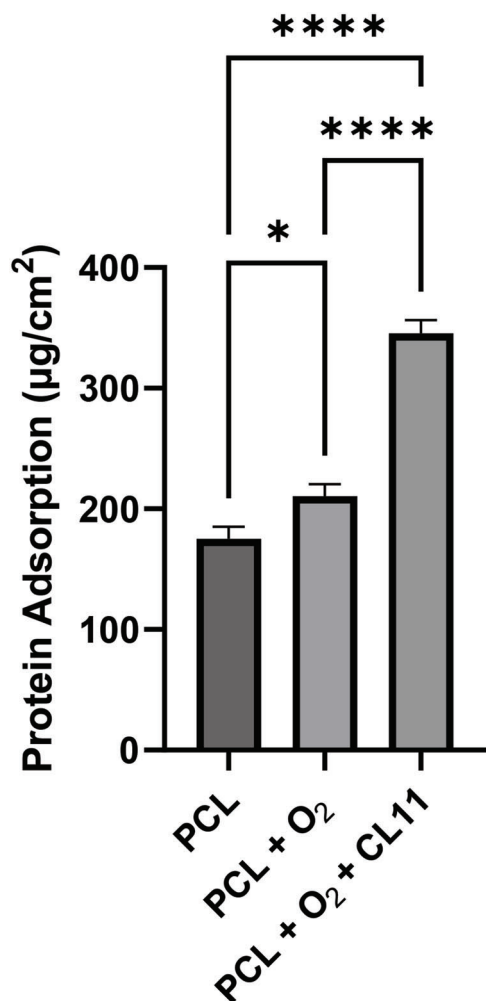


Figure 5. Protein adsorption quantified on the PCL, PCL + oxygen plasma fibers and PCL + oxygen plasma + CL11 fibers ($\mu\text{g cm}^{-2}$) after 24-h incubation (Data presented as mean \pm SD, $n = 3$ independent experiments, three replicates per $n = 1$, and three values taken per sample; * $p < 0.05$ and **** $p < 0.0001$).

and a change in surface roughness.^[10,14,26] However, in this study, the decrease in water contact angle observed is perhaps due to the porosity of the samples. Oxygen plasma and CL11 modifications of PCL were confirmed using XPS analysis. The addition of oxygen plasma to PCL resulted in the addition of oxygen functional groups, and the addition of CL11 to PCL showed the introduction of nitrogen functional groups, as seen in the XPS spectra in Figure 3 and Table 1. Unexpected small traces of silicon were detected on oxygen plasma-treated samples, believed to be a contaminant from the glass vessel used in the oxygen plasma process. The amount of silicon detected increased significantly after the silanization process due to the presence of silicon in 11-aminoundecyltriethoxysilane. Our previous findings have demonstrated that the addition of 11-aminoundecyltriethoxysilane (CL11) to a substrate changes the surface nanotopography, increasing surface roughness.^[14] Changes in nanotopography were confirmed using atomic force microscopy. AFM micrographs (Figure 4) illustrated that modify-

Table 2. R_q , R_a , and Adhesion values of materials quantified from images in Figure 4 (mean \pm SD, $n = 3$; Three replicates per $n = 1$ and three values taken per sample).

Sample	R_q [nm]	R_a [nm]	Adhesion mean [nN]
PCL	55.6 ± 5.3	43.8 ± 1.2	29.1 ± 1.2
PCL + O ₂	96.1 ± 6.5	77.3 ± 3.5	9.9 ± 0.4
PCL + O ₂ + CL11	119.0 ± 4.5	94.3 ± 5.4	11.4 ± 0.9

ing PCL fibers with oxygen plasma and CL11 increased the surface roughness of the polymer, as shown by increasing R_a and R_q values. Modifying PCL with oxygen plasma has been shown to induce surface roughness, as it is suggested that the increase in surface roughness could be due to the bombardment of the surface by energetic particles in the plasma, resulting in etching/degradation of the surface.^[27]

Jeon et al. modified melt-plotted PCL scaffolds with oxygen plasma, which resulted in the formation of nano-sized pits in the surface morphology, leading to increased surface roughness.^[28] Martins et al. also reported an increase in surface roughness when modifying PCL nanofibers with varying oxygen plasma powers and times.^[29] The increase in surface roughness when modifying PCL with CL11 is in line with our previous findings, in which CL11 modification of glass increased surface roughness compared to using APTES.^[14,26] Modifying PCL fibers with oxygen plasma and CL11 changed the adhesive properties of the PCL fibers. The modifications caused a decrease in adhesiveness and the force recorded between the polymer fiber and the AFM cantilever tip made using silicon nitride. Our findings are similar to those published in Tokachichu et al., who observed a decrease in AFM adhesion values when modifying Polydimethylsiloxane (PDMS) discs with oxygen plasma alone and a further decrease in adhesion value when modifying them with a self-assembling monolayer of Perfluorodecyltriethoxysilane.^[30] Movahed et al. also reported a decrease in adhesion values when modifying silicon-incorporated diamond-like coatings with both oxygen and argon plasma, simultaneously reporting an increase in hydrophilicity with the plasma treatments.^[31] This supports our study in which increasing the hydrophilic properties of the PCL fibers using oxygen plasma and CL11 reduces the adhesive forces measured between the polymer and the AFM cantilever tip, which is hydrophobic in nature. The addition of the CL11 to the PCL fibers caused an increase in the elastic modulus of the fibers, a contradictory result to our previous study when modifying glass with CL11, which decreased elastic modulus.^[14] There is much literature to suggest that modifying biomaterials with aminosilanes, such as APTES, advantageously increases mechanical properties of the material. Khan et al. reported an increase in mechanical properties when modifying phosphate glass fibers with 5 and 10 wt.% 3-aminopropyl-triethoxysilane, whereas Sagnella et al. reported a significant increase in silk fibroin mechanical properties when modified with APTES conjugated with a terthiophene T3 fluorophore (MT3).^[32,33] Modifying fibers with oxygen plasma alone showed significant changes in mechanical properties, as observed by Pappa et al. who observed no change in mechanical properties of PCL fibers and those modified with oxygen plasma.^[34]

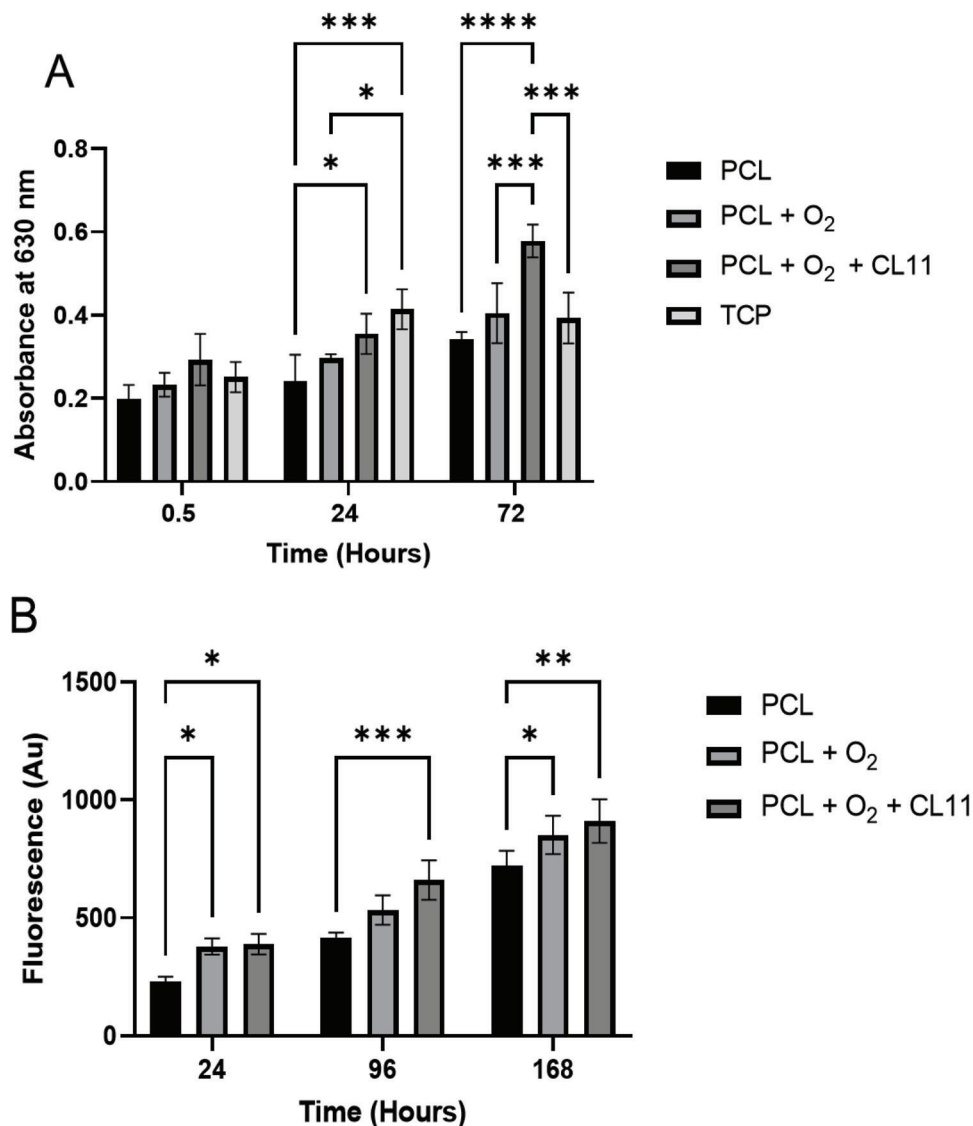


Figure 6. A) Absorbance of eluted crystal violet stain on PCL, PCL + oxygen plasma fibers and PCL + oxygen plasma + CL11 fibers after 0.5, 24, and 72 h in culture. B) Proliferation activity of NG108-15 neuronal cells cultured on PCL, PCL + oxygen plasma fibers and PCL + oxygen plasma + CL11 fibers after 24, 96, and 168 h in culture (Data presented as mean \pm SD, $n = 3$ independent experiments, three replicates per $n = 1$ and three values taken per sample; * $p < 0.05$, ** $p < 0.01$, *** $p < 0.001$, and **** $p < 0.0001$).

Changing the surface wettability and adhesiveness of a polymer, as well as the roughness of its surface, are valuable tools in tissue engineering, as changing surface properties can cause increased protein surface interactions due to increased surface area and rougher surfaces leading to controlling cell attachment, proliferation, and differentiation.^[35,36] This was observed when a protein adsorption assay was performed on the unmodified and modified fibers. The addition of oxygen plasma alone significantly increased total protein adsorption to the fibers. Similar results were observed by Recek et al., who noted a significant increase in protein adsorption using Fetal calf serum on oxygen plasma-treated polyethylene terephthalate substrates compared to unmodified substrates.^[37] Siri et al. observed an increase in laminin protein adsorption on air plasma-treated PCL fibers compared to unmodified surfaces.^[38] Our results also show that

the addition of the CL11 aminosilane, grafted to oxygen plasma treated PCL fibers, significantly increased protein adsorption values. The addition of amines to surfaces via a number of different methods has previously been shown to promote protein adsorption. Omrani et al. modified PCL films by aminolysis using 1, 6-hexanediamine and exhibited higher values of protein attachment compared to unmodified PCL films.^[39] Myung et al., however, reported no statistical differences in FCS protein adsorption when modifying PCL scaffolds with plasma polymerization using allylamine or acrylic acid to fabricate amine groups and carboxyl groups on the surface, respectively, likely due to the complexity of the 3D PCL structures.^[40] In our previous studies, the addition of amine groups using aminosilanes has previously been shown to support protein adsorption to surfaces. Chen et al. noted that when CL11-modified surfaces were cultured with

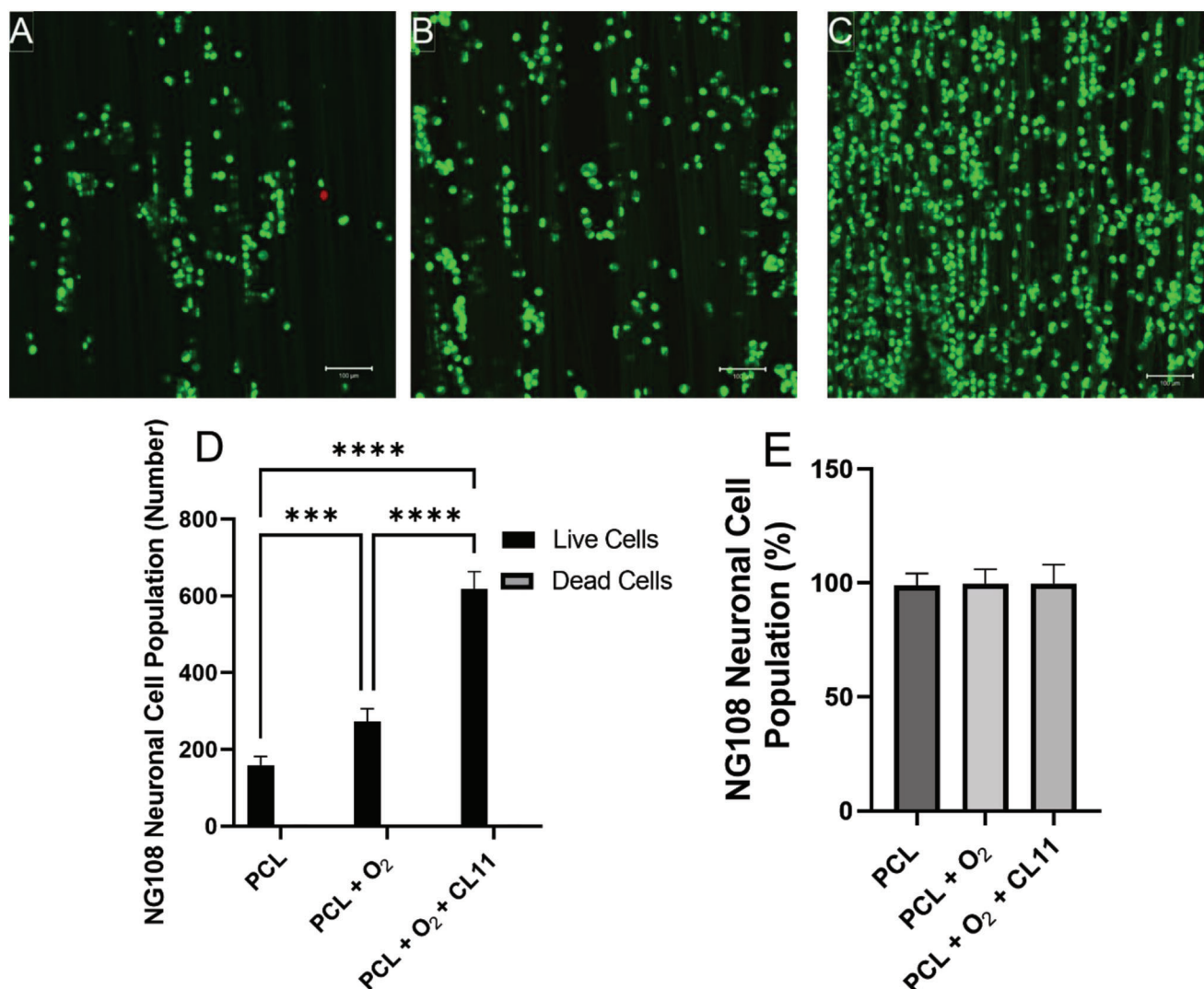


Figure 7. Confocal micrographs illustrating NG108-15 neuronal cell viability cultured on: A) PCL films, B) PCL + oxygen plasma fibers and C) PCL + oxygen plasma + CL11 fibers after 7 days in culture (Scale bar = 100 μ m). Live cells stained with Syto 9 (Green) and dead cells stained with propidium iodide (red). E) Number of live cells versus dead cells per sample and F) live cell analysis expressed as a percentage (Data presented as mean \pm SD, $n = 3$ independent experiments, three replicates per $n = 1$ and three values taken per sample. A total 27 images per sample quantified; * $p < 0.05$ and ** $p < 0.01$).

fibronectin, surfaces exhibited a rougher profile, observed using atomic force microscopy by increased height profiles.^[26] Bassett et al. also observed increased protein adsorption to rougher surfaces when manufacturing blends of P(3HO) and P(3HB).^[41] Interestingly, albumin protein adsorption increased as the hydrophobicity of the surface decreased. Previously, it was suggested that hydrophobic surfaces favored increased protein adsorption; however, many studies report similar amounts of adsorption on both hydrophobic and hydrophilic surfaces.^[42,43] However, in this study, differences in surface chemistry, roughness, and topography are driving increased and conformationally correct protein adsorption, as evidenced by the cell responses.

Modified PCL fibers better supported NG108-15 neuronal cell adhesion, proliferation, and viability compared to unmodified PCL fibers, as shown in cell adhesion, proliferation, and live/dead assays. NG108-15 neuronal cells are commonly used in nerve tis-

sue engineering research as a proxy for nerve regeneration in vitro as they are indicative of primary neuron responses.^[14,44] Significantly higher numbers of live cells were observed adhering to CL11 modified PCL fibers, compared to oxygen plasma modified and unmodified PCL fibers, after 7 days. This aligns with the significant increase in NG108-15 neuronal cell adhesion after 72 h in culture and the increase in cell proliferation activity after 24, 96, and 168 h.

Our previous findings demonstrated an increase in NG108-15 neuronal cell attachment and viability of CL11-modified glass substrates compared to unmodified glass substrates.^[14] The addition of amine groups to surfaces has previously been shown to increase neuronal cell attachment and viability.^[8] The addition of oxygen plasma to unmodified PCL fibers better supported NG108-15 neuronal cell attachment compared to unmodified surfaces. Oxygen plasma has been shown to increase neuronal

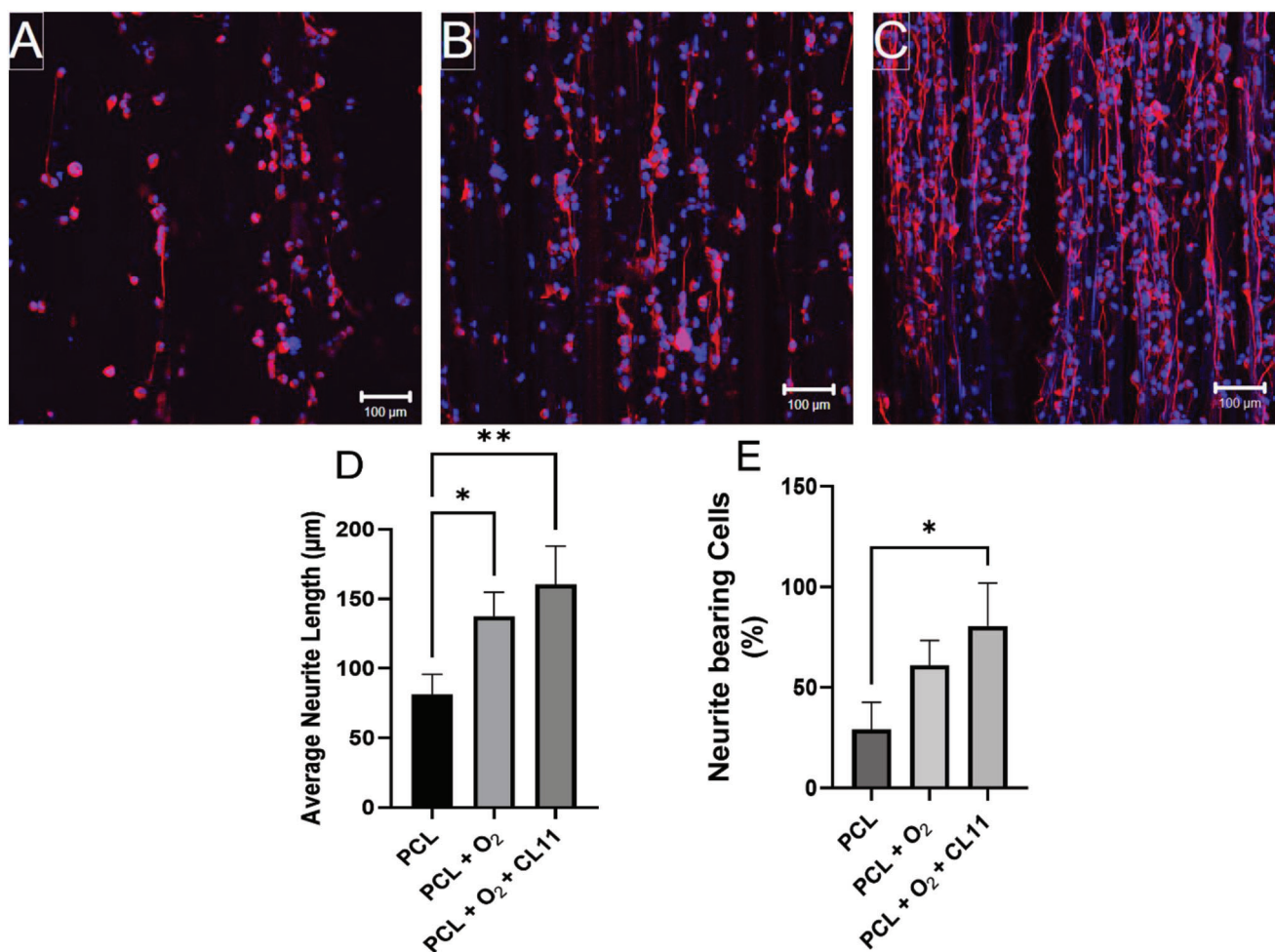


Figure 8. Confocal micrographs of NG108-15 neuronal cells immunolabeled for neurites marked β III-tubulin (red) and cell nucleus stain DAPI (blue) on: A) PCL films, B) PCL + oxygen plasma fibers and C) PCL + oxygen plasma + CL11 fibers (Scale bar = 100 μ m). D) Average neurite length per condition after 7 days in culture and E) the percentage of neurite bearing neuronal cells (Data presented as mean \pm SD, n = 3 independent experiments, three replicates per n = 1 and three values taken per sample. A total 27 images per sample quantified; * p < 0.05 and ** p < 0.01).

cell adhesion to substrates. Hoshino et al. demonstrated that the addition of oxygen plasma to parylene-C surfaces resulted in increased PC12 adhesiveness.^[45] Khorasani et al. also observed an increase in B65 nervous tissue cells to oxygen plasma-treated PLLA and PLGA films compared to unmodified films.^[46] The addition of both reactive groups, amine and oxygen, to PCL fibers increases surface roughness, as seen in Figure 3 and Table 1, leading to greater protein adsorption and therefore increased cell adhesion.^[47]

Modifying PCL with oxygen plasma and CL11 significantly supported NG108-15 neuronal cell differentiation across the scaffolds, as seen in an increase in the average neurite lengths measured as well as increased numbers of cells bearing neurites. Our results suggest that changing the surface topography, surface chemistry, and mechanical properties of PCL using both modifications can support and guide NG108-15 neuronal cell neurite outgrowth by providing physical guidance cues.^[48] Our findings are in line with previous findings that suggest modifying biomaterials for nerve repair with oxygen plasma can induce neuronal cell differentiation. Jahani et al. modified PCL

nanofibers with oxygen plasma and differentiated mesenchymal stem cells into neural-like cells that expressed neuronal markers β III tubulin, Nestin, and MAP2.^[49] Significantly longer neurites and cells bearing neurites were observed when using both oxygen plasma and CL11 modification together compared to oxygen plasma and PCL alone. Hopper et al. observed that the addition of amine-functionalized nanodiamonds to glass substrates significantly increased NG108-15 neuronal cell neurite outgrowth length and increased the number of cells outgrowing neurites.^[8] Joseph et al. also reported that amino group presenting SAM surfaces demonstrated greater potential to support neurite outgrowth from rat neurospheres compared to other SAM-coated coverslips.^[13] Neuronal cell differentiation can also be induced by changes to surface roughness and topography. Li et al. reported that human iPSC differentiation into neural progenitor cells could be controlled using different degrees of surface roughness.^[50] Lizarraga-Valderrama et al. also demonstrated that rougher surfaces induced NG108-15 neuronal cell differentiation when incorporating varying amounts of bioglass particles into polyhydroxyalkanoate solvent-cast films.^[51] Changes to

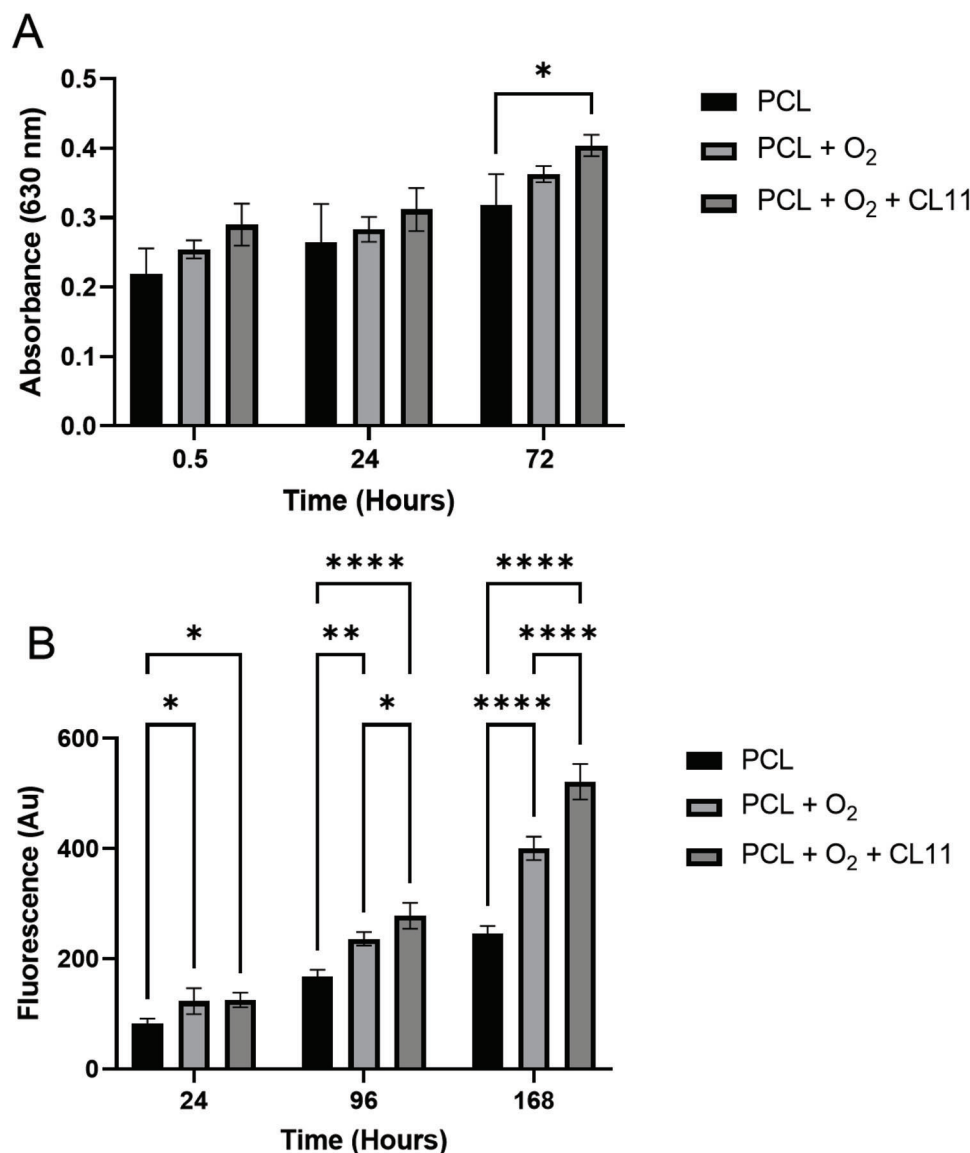


Figure 9. A) Absorbance of eluted crystal violet stain, from rat primary Schwann cells cultured on PCL, PCL + oxygen plasma fibers, and PCL + oxygen plasma + CL11 fibers after 0.5, 24, and 72 h in culture. B) Proliferation activity of rat primary Schwann cells cultured on PCL, PCL + oxygen plasma fibers, and PCL + oxygen plasma + CL11 fibers after 24, 96, and 168 h in culture (mean \pm SD, $n = 3$ independent experiments; * $p < 0.05$, ** $p < 0.01$, and **** $p < 0.0001$).

mechanical properties can also induce and guide neurite elongation in NG108-15 neuronal cells.^[52] Leach et al. exhibited longer, more branched neurites extending from PC12 neuronal cells on stiff substrates (10^2 – 10^4 Pa) compared to softer substrates of 10 Pa, whereas Kayal et al. did not observe any effect on neurite outgrowth length from NG108-15 neuronal cells when culturing cells on stiff and soft substrates.^[52,53]

Viable Schwann cell attachment to a nerve scaffold is absolutely crucial for successful peripheral nerve regeneration to occur, for proliferation of Schwann cells to form the Bands of Büngner, and for mature Schwann cells to re-myelinate regenerating nerve fibers.^[54]

Aligned PCL fibers, unmodified and modified, supported primary Schwann cell adhesion, proliferation, and viability. How-

ever, significant increases in cell adhesion, proliferation, and viability were observed with the addition of oxygen plasma and CL11 aminosilane.

An increase in live Schwann cell attachment was observed when using oxygen plasma and CL11 modifications. Similar results were observed in the study by Prabhakaran et al., who observed an increase in RT4-D6P2T Schwann cell proliferation on air plasma-modified PCL fibers compared to unmodified fibers.^[55] Huang et al. reported that modifying chitosan-PLGA films with oxygen plasma led to an increase in laminin adsorption compared to modifying films with argon plasma, which ultimately led to an increase in attachment and proliferation of rat primary Schwann cells.^[53] Mechanical cues can also guide Schwann cell attachment, as seen in Rosso et al.,

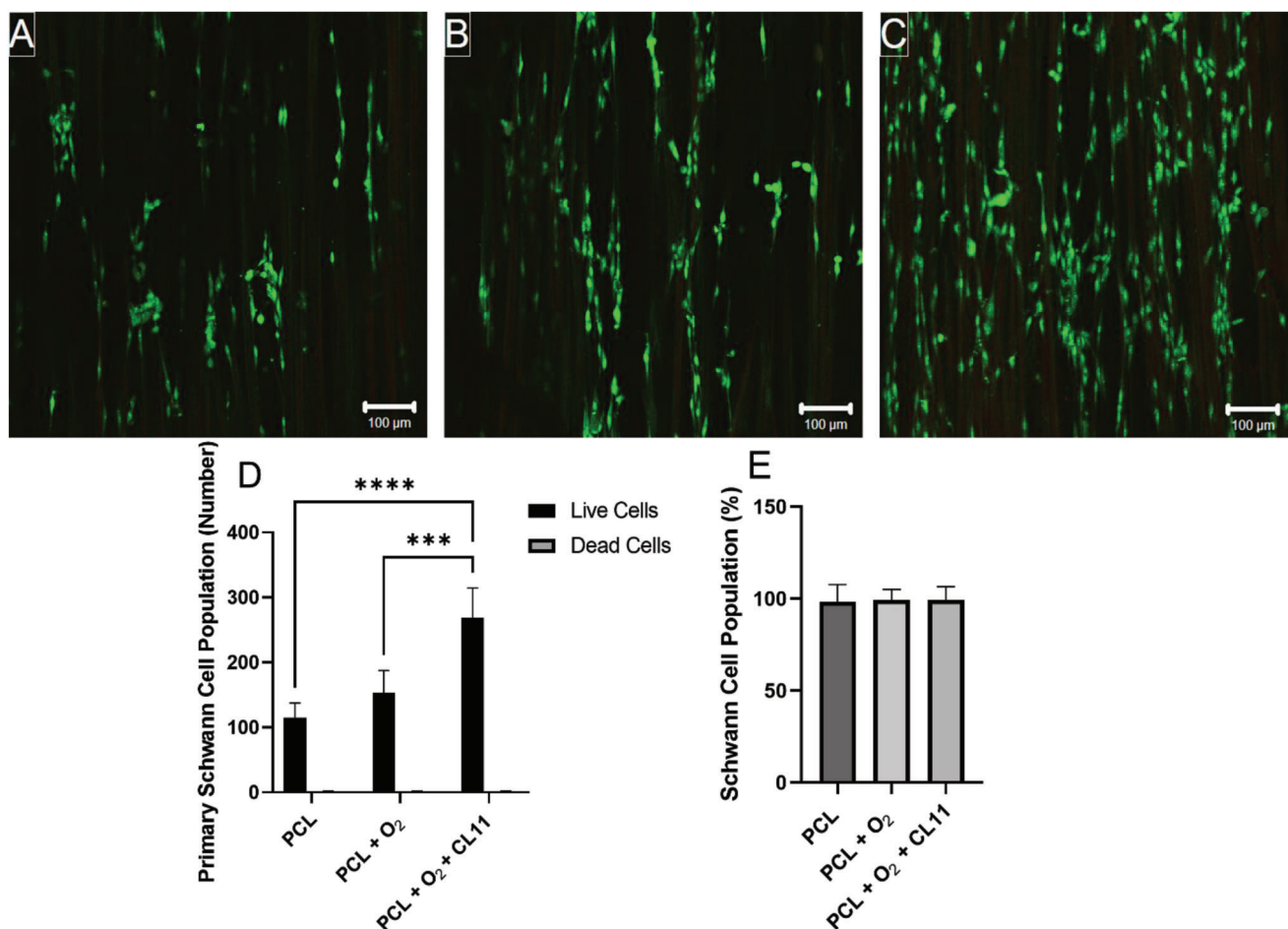


Figure 10. Confocal micrographs illustrating primary Schwann cell viability cultured on: A) PCL films, B) PCL + oxygen plasma fibers and C) PCL + oxygen plasma + CL11 fibers (Scale bar = 100 μ m). Live cells were stained with Syto 9 (green) and dead cells labeled with propidium iodide (red). D) Number of live cells versus dead cells per sample and E) live cell analysis expressed as percentage (Data presented as mean \pm SD, $n = 3$ independent experiments, three replicates per $n = 1$ and three values taken per sample. A total 27 images per sample quantified, **** $p < 0.0001$).

who noted significant primary Schwann cell attachment from DRGs on substrates of 20 KPa compared to softer substrates of 1–10 KPa.^[56]

All scaffolds supported Schwann cell attachment, and cells stained positive for S100 β antigens. Schwann cells aligned themselves to the fibers in a typical elongated morphology, as seen in Figure 8A–C, and no differences were detected between the average Schwann lengths measured (Figure 8D). However, with regard to aspect ratio (width:length), Schwann cells cultured on oxygen plasma and CL11-modified scaffolds had a significantly higher aspect ratio recorded compared to unmodified PCL scaffolds, indicating a more mature phenotype as seen in vivo. Similar observations have been noted in other studies, suggesting the addition of amine groups to surfaces supports and maintains Schwann cell phenotype.^[14]

Hopper et al. reported polygonal-shaped Schwann cells on acrylic acid-coated surfaces, whereas mature Schwann cell phenotypes and elongated cells were observed on amine-functionalized nano-diamond surfaces.^[8] Li et al. also reported no change in Schwann cell phenotype on silanized chitosan scaffolds compared to unmodified chitosan scaffolds.^[12]

E13 chick DRGs were isolated, as previously described,^[7] and placed onto modified and unmodified PCL scaffolds that had been inserted into NGC lumens in a novel 3D ex vivo testing system to mimic a peripheral nerve injury.^[6] This study opted to use embryonic chick DRG explants to obtain results indicative of the in vivo response and reduce animal use (in line with the 3Rs).^[57] The addition of both oxygen plasma and CL11 modification to PCL scaffolds significantly promoted increased axonal outgrowth length and Schwann cell migration distances from embryonic chick dorsal root ganglia explants, with longer axon outgrowth and further Schwann cell migration observed on CL11 modified scaffolds. Similar results were observed in Sandoval-Castellano et al., who observed an increase in axon outgrowth length and Schwann cell migration distances from E13 chick DRGs on air plasma-treated PCL scaffolds compared to unmodified PCL scaffolds.^[7] However, no difference was observed when comparing amine group modified PCL scaffolds with air plasma-modified scaffolds using single modifications. It is likely that the addition of two modifications to one scaffold (oxygen plus CL11) in our work is causing the significant increase in axon outgrowth length in chick DRGs. This was

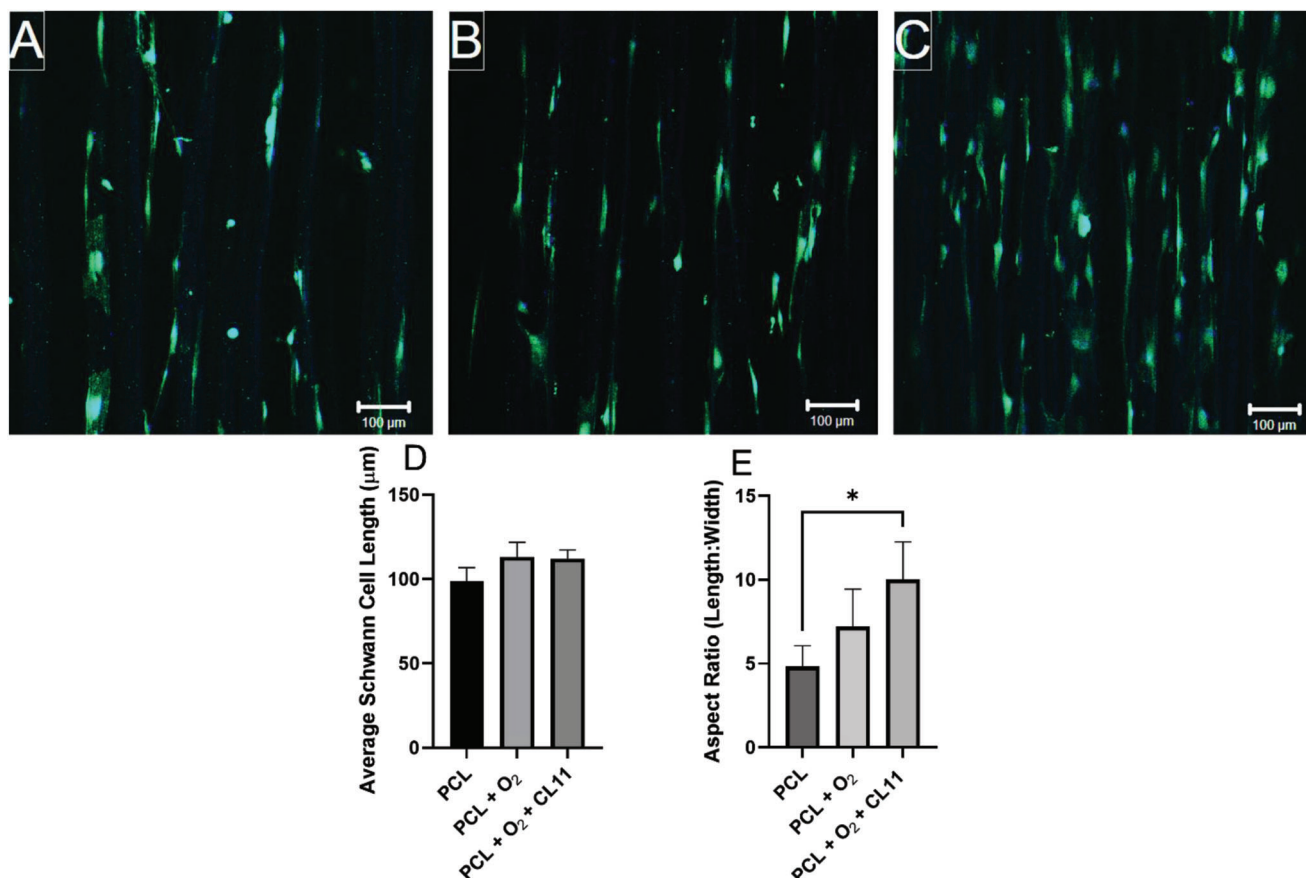


Figure 11. Confocal micrographs of primary Schwann cells immunolabeled for Schwann cell marker S100β (green) and cell nucleus stain DAPI (blue), to confirm Schwann cell phenotype, on: A) PCL films, B) PCL + oxygen plasma fibers and C) PCL + oxygen plasma + CL11 fibers (Scale bar = 100 μm). D) Average Schwann cell length; E) aspect ratio (length/width) to identify Schwann cell phenotype (Data presented as mean ± SD, $n = 3$ independent experiments, three replicates per $n = 1$ and three values taken per sample. A total 27 images per sample quantified and 100 cells measured per condition for width and length; * $p < 0.05$).

observed in Sandoval-Castellano et al. when PCL was modified with allylamine plasma, heparin, and the addition of nerve growth factor and brain-derived neurotrophic factor, indicating a need for multiple modifications.^[7] Similar results were seen in Hopper et al., in which longer neurites were observed from primary neurons cultured on acrylic acid and amine-functionalized nano-diamond surfaces compared to neurons cultured on plain glass and poly-L-lysine coated glass substrates.^[8] DRGs have also been reported to be mechanosensitive. Rosso et al. reported longer neurites from embryonic DRGs on stiffer substrates (20 KPa) compared to softer substrates of 1–10 KPa.^[52,56] This work demonstrates that changing surface chemistry, surface topography, roughness, and mechanical stiffness all contribute to changes in neuronal and Schwann cell adhesion, proliferation, viability, and differentiation, providing sub-micron guidance cues. However, the limitations of this work are the in vivo response to the CL11 addition and the efficacy of the CL11 addition after sterilization using conventional methods for medical devices, such as UV and gamma irradiation. Therefore, further work will investigate the effect and degradation of the silane in vivo, the effects of sterilization, and the in vivo response.

4. Conclusion

In summary, in this work we have developed a surface deposition method resulting in the addition of two modifications, oxygen plasma and CL11, to PCL aligned fiber scaffolds that significantly change the surface chemistry and topography of PCL by decreasing the water contact angle, changing surface energy properties, adding reactive chemical groups, and significantly increasing surface roughness and adhesion. These changes in surface chemistry and topography, at the submicron scale, have significantly supported NG108-15 neuronal cells, primary Schwann cells, axon outgrowth, and Schwann cell migration from dorsal root ganglia explants. The CL11 modification of glass substrates has been extensively characterized for nerve tissue engineering applications^[14] and bone tissue engineering.^[26] This is the first study to modify biomaterials using an aminosilane other than APTES for tissue engineering applications and the first to use CL11 modification for peripheral nerve repair. Our study and previous studies indicate that by using a longer-chain aminosilane, surface topography, chemical deposition, and cell behavior can be influenced and controlled at the submicron scale.^[10,14,26]

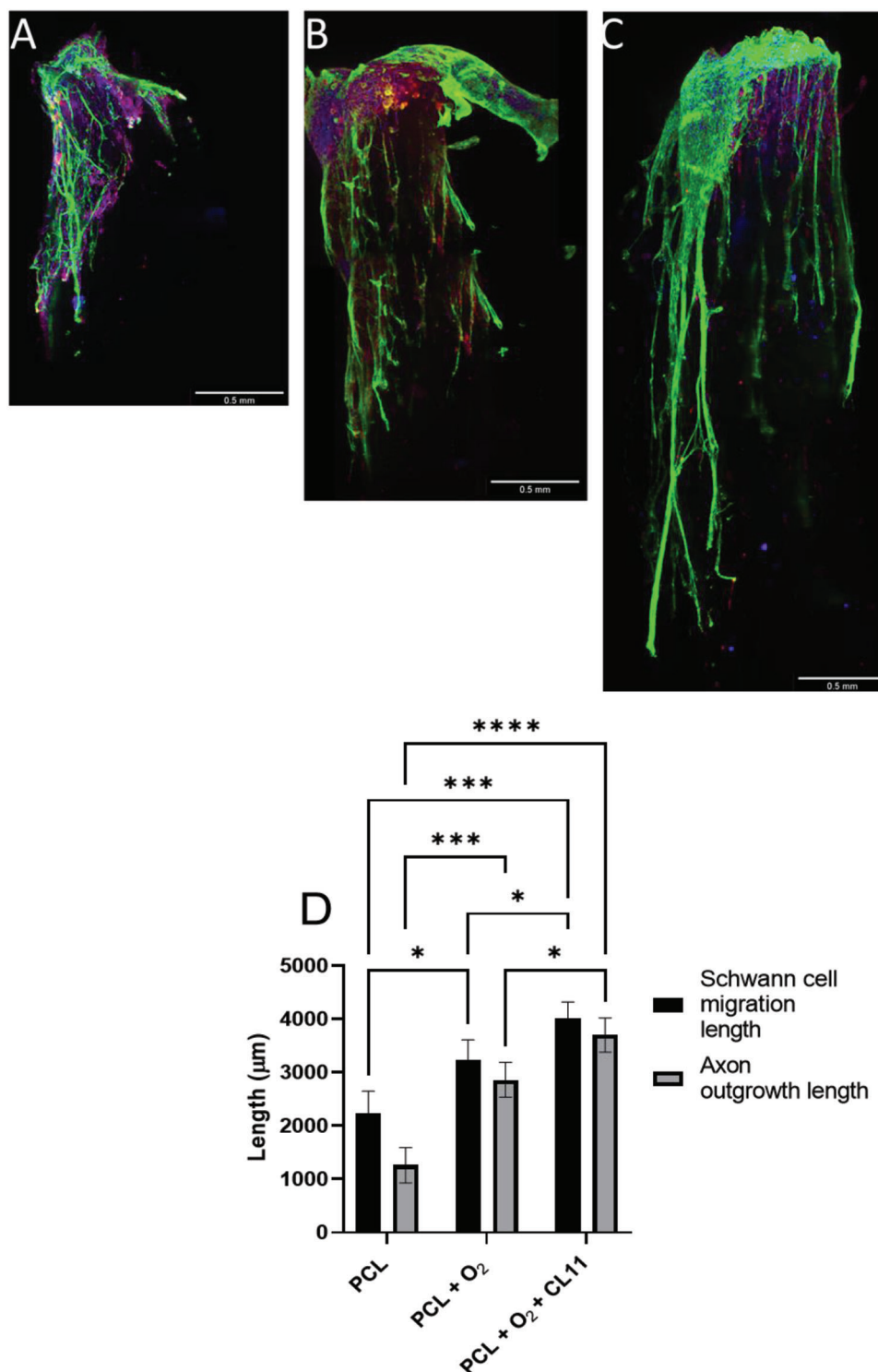


Figure 12. Light sheet micrographs of embryonic chick DRG explants on fibers immunolabeled for axon outgrowth marker β III tubulin (green), Schwann cell marker S100 β (red) and cell nucleus stain DAPI (blue) on: A) PCL films, B) PCL + oxygen plasma fibers and C) PCL + oxygen plasma + CL11 fibers (Scale bar = 0.5 mm). D) Schwann cell migration length and average neurite outgrowth length was determined from Light sheet micrographs (Data presented as mean \pm SD, $n = 3$ independent experiments, three replicates per $n = 1$ and a total of 9 DRGs per condition analyzed; * $p < 0.05$, *** $p < 0.001$, and **** $p < 0.0001$).

Silane modification is also a scalable and cost-effective tool to modify biomaterials with a variety of chemical reactive groups for many different applications in tissue engineering. The technology is simple and can be easily translated to a range of different medical devices. Furthermore, amino-silanization of biomaterials can lead to further modifications, such as the addition of bioactive molecules onto surfaces, such as growth factors, drug therapies, and anti-microbial agents, such as the binding of heparin through its amine linkage.^[12]

5. Experimental Section

Fabrication of PCL Scaffolds: Aligned fiber PCL scaffolds, 10 μm in diameter, were fabricated via electrospinning as per the methods previously described.^[7] Briefly, Polycaprolactone (PCL, M_n 80 000 g mol^{-1} , Merck) was dissolved in Dichloromethane (DCM, Fisher Scientific) at 37 °C to form a 20 w/v% solution. The solution was ejected from a 1 mL (Beckton Dickinson, BD) syringe at a rate of 9 mL h^{-1} using a syringe pump (AL 1000–220, World Precision Instruments, WPI), at a voltage of 21 kV. Fibers were collected on aluminum foil, wrapped around a rotating cylindrical mandrel (6 cm in diameter) attached to a motor (IKA Works).^[20]

Characterization of PCL Scaffolds: The characterization of PCL scaffolds was performed as previously described.^[20] Briefly, fibers were cut into small segments and sputter coated with 20 nm thick gold (SC 500A, Emscope) prior to imaging using a field emission SEM (Sorby Centre, FE SEM JSM-6500F, Jeol Ltd.).^[7] Images were analyzed using National Institutes of Health (NIH) Image J software for fiber diameter and fiber alignment.^[57,58]

Silane Modification of PCL Scaffolds: PCL-coated substrates were treated with oxygen plasma at 20 W for 5 min (Henniker Plasma HPT-100). In a fresh vessel, plasma-treated substrates were then submerged in a solution of 2% v/v 11-aminoundecyltriethoxysilane (Fluorochem S25045) in isopropanol for 1 h to modify the surfaces. Samples were rinsed in isopropanol, then washed in isopropanol on a rocker plate for 3 min, twice. Samples were dried and kept under vacuum to limit the potential for oxidation.^[14,59]

Water Contact Angle Measurement: Directly following the silanization process detailed as above in Section 1, water contact angle measurements were carried out using the sessile drop method on an Attension Theta Lite Optical Tensiometer (TL100, Attension, Biolin Scientific, Finland).^[14] Three technical repeats were used for each measurement, with 10 replicate measurements taken across the surface of 2 cover slips (5 measurements from each). Infra-red images of the droplets were recorded at 15 fps for 10 s and analyzed using One-Attension software. Exported data was averaged using MATLAB r2019a, following purpose-written code.^[14]

X-Ray Photoelectron Spectroscopy: Samples were prepared as above.^[14] As soon as practicable, following drying (within 24 h), samples were analyzed using XPS as previously described.^[26] Briefly, a Kratos Axis Ultra DLD spectrometer was used to perform XPS analysis using a monochromated AlK α X-ray (1486.6 eV).^[26] Three spots of each sample were recorded below 5×10^{-8} Torr, and a total of four repeats were analyzed to determine the relative atomic percent concentration, calculated using CasaXPS version 2.3.15 software.^[26]

Atomic Force Microscopy: AFM microscopy was performed in a tapping model with SCANASYST-AIR probes under ambient conditions on a Bruker Dimension Icon AFM. PCL fibers, modified and unmodified, were cast onto cover glasses and then stuck to a magnetic AFM support. Different areas of the samples were then analyzed and characterized in Bruker NanoScope Analysis software (Version 2.0). The data were further averaged weight-dependently on the surface area measured to obtain accurate roughness R_q (Root Mean Squared Roughness) and R_a (Roughness Average) and adhesion values (how adhesive the polymer fiber is to the tip of the AFM cantilever). Mechanical analysis was performed by fitting data with the Derjaguin–Muller–Toporov (DMT) model to determine the elastic modulus of modified and unmodified fibers, as previously described.^[14]

Protein Adsorption Assay: A protein adsorption assay was performed on fiber scaffolds to determine the amount of adsorbed proteins from undiluted fetal bovine serum (FBS), as previously described.^[41] Briefly, fiber scaffolds were cut into 10 mm \times 10 mm squares and incubated with 400 μL of undiluted FBS at 37 °C for 24 h.^[41] Samples were washed once with PBS, removed and placed into a new well plate. One milliliter of 2% sodium dodecyl sulfate (SDS) in PBS was added to each scaffold for 24 h at room temperature, under shaking conditions. A Bicinchoninic acid assay was then performed to measure absorbance at 562 nm.^[41]

NG108-15 Neuronal Cell Culture: NG108-15 (ECACC 88112303) neuronal cells were cultured and used between passages 12–15 for experiments. Experimental culture and conditions were used as previously described.^[20] Cultures were maintained for 7 days, changing the culture medium to serum free Dulbecco's Modified Eagle Medium (DMEM) after 2 days in culture.^[14]

Schwann Cell Isolation and Culture: To isolate primary Schwann cells for experiments, an adult male Wistar rat (10–12 weeks old) was sacrificed by Schedule 1 according to local regulations and the regulation of the Animals (Scientific Procedures) Act 1986.^[60] Briefly, sciatic nerves were isolated, the epineurium removed, and tissue mechanically and enzymatically dissociated to digest tissue and passed through a 2 μm cell sieve to isolate primary Schwann cells.^[60] Cells were cultured in specialized Dulbecco's Modified Eagle Medium (DMEM) containing D-Valine to inhibit fibroblasts growth and obtain a pure culture of Schwann cells.^[60] Once pure, 60 000 rat primary Schwann cells were seeded and cultured onto fibers for 7 days in Dulbecco's Modified Eagle Medium (DMEM) containing 5 μM Forskolin (Merck). The medium was changed on day 4 in culture.^[14,60]

Dorsal Root Ganglia Isolation: Dorsal root ganglia (DRG) from embryonic chicks were isolated as previously described.^[25] Briefly, fertilized brown chicken eggs (Henry Stewart & Co. Ltd.) were incubated at 37.5 °C and 50–70% humidity for 13 days. E13 embryos were cleaned, and organs were removed to observe the spinal column and cord. DRGs were collected and placed into a petri dish containing warm DMEM media.^[25]

Ex Vivo 3D Testing of Modified and Unmodified PCL Fibres: Unmodified and modified PCL fibers were threaded into 3D-printed Polyethylene Glycol (PEG) tubes as previously described.^[6] Briefly, PEG tubes containing PCL fibers were placed into tube holders on a metal grid in a 6 well plate. Isolated chick DRGs were placed into fibers in PEG tubes and left to attach for 20 min. Well plates were then filled with Dulbecco's Modified Eagle Medium (DMEM), and DRGs were left in culture for 7 days at 37 °C and 5% CO_2 .⁶

Cell Adhesion Assay: Cell adhesion on the modified and unmodified scaffolds was determined using a crystal violet cell adhesion assay after 0.5, 24, and 72 h. First of all, 30 000 NG108-15 neuronal cells and 60 000 rat primary Schwann cells were seeded onto scaffolds and left to attach at 37 °C and 5% CO_2 . At each respective time-point, culture medium was removed and cells were fixed using 3.7% paraformaldehyde for 20 min at room temperature. Samples were transferred to a new 24 well plate and stained with a 0.2% crystal violet solution (w/v Sigma, UK, in 10% (v/v) ethanol (Fisher Scientific, UK) for 10 min at room temperature. Samples were then washed twice with PBS followed by the addition of a 10% acetic acid solution, in deionized water to elute the stain from the cells. This solution was transferred to a 96-well plates, and the absorbance was read at 630 nm using a Bio-Tek ELx 800 absorbance microplate reader.^[61]

Cell Proliferation Assay: The proliferation activity of the NG108-15 neuronal cells, on the unmodified and modified PCL scaffolds, was determined using a resazurin assay as previously described.^[62] Briefly, at relevant time points, 24, 96, and 168 h, culture medium was removed, and samples were cultured in a 100 μM resazurin salt in PBS solution for 4 h at 37 °C and 5% CO_2 .^[62] The reduced formazan product was transferred to a black 96-well plate, in triplicate, and the fluorescence was read in a FLx800 fluorescence plate reader (Biotek Instruments Inc.) at 540/635 nm.^[62]

Live/Dead Analysis: Live/dead analysis was performed on NG108-15 neuronal and Schwann cells after 7 days in culture, as previously described.^[20] Briefly, culture medium was removed and replaced with serum-free-medium including 0.001% Syto-9 (Invitrogen) and 0.0015% propidium iodide (Invitrogen) for 30 min at 37 °C and 5% CO_2 .^[20] Images were taken on a Zeiss 510 upright confocal. Live and dead cells were

counted using ITCN cell counter software on National Institutes of Health (NIH) Image J software.^[63] The data were expressed as the number of live versus dead cells and a percentage of cell viability \pm SD.

Immunolabelling of NG108-15 Neuronal Cells, Primary Schwann Cell, and Chick DRG Neurite Growth: NG108-15 neuronal cells and neurites outgrown from DRG explants, were labeled for β III-tubulin to assess neurite outgrowth as a proxy of nerve regeneration. Briefly, cells were fixed with 3.7% (v/v) paraformaldehyde for 20 min, cell walls broken down with 0.1% Triton X-100 for 45 min, and unreactive binding sites blocked with 3% bovine serum albumin in PBS for 30 min, all at room temperature.^[20] NG108-15 neuronal cells and primary neurons from chick DRGs were labeled with a mouse anti- β III-tubulin antibody (1:250 dilution, for 48 h at 4 °C) followed by a Texas Red-conjugated anti-mouse IgG antibody (1:250 dilution, for 90 min at room temperature).^[20] Rat, and chick, primary Schwann cells were fixed, permeabilized, and blocked using the same procedure as above. However, they were labeled with a polyclonal rabbit anti-S100 β (1:250) antibody followed by a FITC-conjugated secondary anti-rabbit IgG antibody (1:100) for 48 h and 90 min, respectively.^[20] 4,6-diamidino-2-phenylindole dihydrochloride (DAPI) was used to label all cell nuclei for 30 min at room temperature.^[20]

Neurite Outgrowth and Primary Schwann Cell Morphology Assessment: Two different parameters were analyzed to assess NG108-15 neuronal cell differentiation: average neurite length and percentage of cells with neurites.^[20] Images were taken using a 510 Zeiss upright confocal, and three fields of view were taken per sample to obtain images: two from the sides and one from the middle of the sample. A total of 27 images, over three independent experiments, were analyzed. Images were analyzed using Image J (NIH), and neurites were traced using Neuron J plugin tracer software from the cell body to the neurite tip.^[64] The average Schwann cell length and aspect ratio were calculated as previously described^[65] using the ruler tool on NIH Image J.^[57,58] A total of 100 neurites were measured to determine the average neurite length, and a total of 100 Schwann cells were measured for width and length to calculate the average Schwann cell length and aspect ratio.^[20]

Statistical Analysis: GraphPad Instat (GraphPad Software, USA) was used to perform statistical analysis.^[14] One-way analysis of variance (ANOVA; $p < 0.05$) was conducted to analyze the differences between data sets, incorporating Tukey's multiple comparisons test if $p < 0.05$.^[14] Two-way analysis of variance ($p < 0.05$) was conducted to analyze the differences between data sets when assessing live/dead cell numbers, incorporating a Sidak's multiple comparisons test if $p < 0.05$. The data were reported as mean \pm SD, $p < 0.05$.^[14] Each experiment was performed three independent times with each sample repeated three times as $n = 3$, unless otherwise stated differently.^[14]

Acknowledgements

The authors acknowledge the University of Sheffield and the University of Liverpool for funding. The authors wish to acknowledge the Henry Royce Institute for Advanced Materials, funded through EPSRC grants EP/R00661X/1, EP/S019367/1, EP/P02470X/1, and EP/P025285/1, for Light sheet microscope access at the University of Sheffield. The authors would also like to thank Dr Mehri Behbehani and Dr Nicola Green for help with Light sheet microscopy and Dr Alice Pyne for the use of the Bruker Dimension Icon AFM. C.S.T manufactured PCL fiber scaffolds and performed analysis. J.B and M.P performed oxygen plasma and CL11 modification to PCL scaffolds. J.B performed water contact analysis. S.H performed XPS analysis of fibers. D.A.G performed AFM analysis of fibers. C.S.T performed 2D and 3D in vitro cell culture of fibers and performed data analysis. C.S.T wrote the manuscript. J.B and D.A.G contributed to sections of the manuscript. R.D and I.R contributed to funds and edited the manuscript. J.C and J.W. Haycock mobilized funds, conceived the idea, and edited the approved the manuscript.

Conflict of Interest

The authors declare no conflict of interest.

Data Availability Statement

The data that support the findings of this study are available from the corresponding author upon reasonable request.

Keywords

aminosilanes, electrospun fibers, nerve regeneration, peripheral nerves, silane modification, topographical guidance

Received: May 20, 2023

Revised: June 13, 2023

Published online:

- [1] J. H. A. Bell, J. W. Haycock, *Tissue Eng., Part B* **2012**, *18*, 116.
- [2] S. Kehoe, X. F. Zhang, D. Boyd, *J. Mater. Sci.: Mater. Med.* **2011**, *22*, 945.
- [3] S. Kehoe, X. F. Zhang, D. Boyd, *Injury* **2012**, *43*, 553.
- [4] W. Daly, L. Yao, D. Zeugolis, A. Windebank, A. Pandit, *J. R. Soc., Interface* **2012**, *9*, 202.
- [5] S. Y. Chew, R. Mi, A. Hoke, K. W. Leong, *Biomaterials* **2008**, *29*, 653.
- [6] M. Behbehani, A. Glen, C. S. Taylor, A. Schuhmacher, F. Claeysens, J. W. Haycock, *Int. J. Bioprint.* **2017**, *4*, 123.
- [7] A. M. Sandoval-Castellanos, F. Claeysens, J. W. Haycock, *Front. Mater.* **2021**, *8*, 734683.
- [8] A. P. Hopper, J. M. Dugan, A. A. Gill, O. J. L. Fox, P. W. May, J. W. Haycock, F. Claeysens, *Biomed. Mater.* **2014**, *9*, 045009.
- [9] M. Buttiglione, F. Vitiello, E. Sardella, L. Petrone, M. Nardulli, P. Favia, R. D'agostino, R. Gristina, *Biomaterials* **2007**, *28*, 2932.
- [10] S. A. Fawcett, J. M. Curran, R. Chen, N. P. Rhodes, M. F. Murphy, P. Wilson, L. Ranganath, J. P. Dillon, J. A. Gallagher, J. A. Hunt, *Calcif. Tissue Int.* **2017**, *100*, 95.
- [11] J. M. Curran, R. Chen, J. A. Hunt, *Biomaterials* **2005**, *26*, 7057.
- [12] G. Li, L. Zhang, C. Wang, X. Zhao, C. Zhu, Y. Zheng, Y. Wang, Y. Zhao, Y. Yang, *Carbohydr. Polym.* **2014**, *101*, 718.
- [13] G. Joseph, R. P. Orme, T. Kyriacou, R. A. Fricker, P. Roach, *ACS Omega* **2021**, *6*, 19901.
- [14] C. S. Taylor, R. Chen, R. D' Sa, J. A. Hunt, J. M. Curran, J. W. Haycock, *J. Biomed. Mater. Res., Part B* **2021**, *109*, 1713.
- [15] C. S. Taylor, M. Behbehani, A. Glen, P. Basnett, D. A. Gregory, B. B. Lukaszewicz, R. Nigmatullin, F. Claeysens, I. Roy, J. W. Haycock, *ACS Biomater. Sci. Eng.* **2023**, *9*, 1472.
- [16] S. Bose, S. F. Robertson, A. Bandyopadhyay, *Acta Biomater.* **2018**, *66*, 6.
- [17] M. A. Woodruff, D. W. Huttmacher, *Prog. Polym. Sci.* **2010**, *35*, 1217.
- [18] J. M. Corey, D. Y. Lin, K. B. Mycek, Q. Chen, S. Samuel, E. L. Feldman, D. C. Martin, *J. Biomed. Mater. Res., Part A* **2007**, *83A*, 636.
- [19] Y.-T. Kim, V. K. Haftel, S. Kumar, R. V. Bellamkonda, *Biomaterials* **2008**, *29*, 3117.
- [20] M. F. B. Daud, K. C. Pawar, F. Claeysens, A. J. Ryan, J. W. Haycock, *Biomaterials* **2012**, *33*, 5901.
- [21] R. Jirkovec, J. Erben, P. Sajdl, J. Chaloupek, J. Chvojka, *Mater. Des.* **2021**, *205*, 109748.
- [22] S. H. Tan, N.-T. Nguyen, Y. C. Chua, T. G. Kang, *Biomicrofluidics* **2010**, *4*, 032204.
- [23] M. Sivan, D. Madheswaran, M. Asadian, P. Cools, M. Thukkaram, P. Van Der Voort, R. Morent, N. De Geyter, D. Lukas, *Surf. Coat. Technol.* **2020**, *399*, 126203.
- [24] A. Mathur, P. Loskill, S. Hong, J. Y. Lee, S. G. Marcus, L. Dumont, B. R. Conklin, H. Willenbring, L. P. Lee, K. E. Healy, *Stem Cell Res. Ther.* **2013**, *4*, S14.

- [25] A. M. Sandoval-Castellanos, F. Claeysens, J. W. Haycock, *Biotechnol. Bioeng.* **2020**, *117*, 3124.
- [26] R. Chen, J. A. Hunt, S. Fawcett, R. D'sa, R. Akhtar, J. M. Curran, *J. Biomed. Mater. Res., Part A* **2018**, *106*, 1862.
- [27] A. Mozaffari, M. P. Gashti, *Biomedicines* **2022**, *10*, 617.
- [28] H. Jeon, H. Lee, G. Kim, *Tissue Eng., Part C* **2014**, *20*, 951.
- [29] A. Martins, E. D. Pinho, S. Faria, I. Pashkuleva, A. P. Marques, R. L. Reis, N. M. Neves, *Small* **2009**, *5*, 1195.
- [30] D. R. Tokachichu, B. Bhushan, *IEEE Trans. Nanotechnol.* **2006**, *5*, 228.
- [31] S. Movahed, A. K. Nguyen, P. L. Goering, S. A. Skoog, R. J. Narayan, *Biointerphases* **2020**, *15*, 041007.
- [32] R. A. Khan, A. J. Parsons, I. A. Jones, G. S. Walker, C. D. Rudd, *J. Thermoplast. Compos. Mater.* **2011**, *24*, 517.
- [33] A. Sagnella, M. Zambianchi, M. Durso, T. Posati, A. D. Rio, A. Donnadio, A. Mazzanti, A. Pistone, G. Ruani, R. Zamboni, V. Benfenati, M. Melucci, *RSC Adv.* **2015**, *5*, 63401.
- [34] A. M. Pappa, V. Karagkiozaki, S. Krol, S. Kassavetis, D. Konstantinou, C. Pitsalidis, L. Tzounis, N. Pliatsikas, S. Logothetidis, S. Beilstein, *J. Nanotechnol.* **2015**, *22*, 254.
- [35] T. Akkas, C. Citak, A. Sirkecioglu, F. S. Güner, *Polym. Int.* **2013**, *62*, 1202.
- [36] P. Roach, D. Farrar, C. C. Perry, *J. Am. Chem. Soc.* **2005**, *127*, 8168.
- [37] N. Recek, M. Jaganjac, M. Kolar, L. Milkovic, M. Mozetic, K. Stana-Kleinschek, A. Vesel, *Mols* **2013**, *18*, 12441.
- [38] S. Siri, P. Wadbua, V. Amornkitbamrung, N. Kampa, S. Maensiri, *Mater. Sci. Technol.* **2010**, *26*, 1292.
- [39] M. M. Omrani, N. Kiaie, M. Ansari, S. S. Kordestani, *J. Macromol. Sci., Part B: Phys.* **2016**, *55*, 617.
- [40] S. W. Myung, Y. M. u Ko, B. H. Kim, *Jpn. J. Appl. Phys.* **2014**, *53*, 11RB01.
- [41] P. Basnett, K. Y. Ching, M. Stolz, J. C. Knowles, A. R. Boccaccini, C. Smith, I. C. Locke, T. Keshavarz, I. Roy, *React. Funct. Polym.* **2013**, *73*, 1340.
- [42] T. R. Kyriakides, S. F. Badylak, in *Host Response to Biomaterials*, Academic Press, Oxford **2015**, pp. 81–116.
- [43] C. J. Wilson, R. E. Clegg, D. I. Leavesley, M. J. Percy, *Tissue Eng.* **2005**, *11*, 1.
- [44] S. J. Armstrong, M. Wiberg, G. Terenghi, P. J. Kingham, *Tissue Eng.* **2007**, *13*, 2863.
- [45] T. Hoshino, I. Saito, R. Kometani, K. Samejima, S. Matsui, T. Suzuki, K. Mabuchi, Y. X. Kato, *J. Biosci. Bioeng.* **2012**, *113*, 395.
- [46] M. T. Khorasani, H. Mirzadeh, S. Irani, *Radiat. Phys. Chem.* **2008**, *77*, 280.
- [47] B. Lukasiewicz, P. Basnett, R. Nigmatullin, R. Matharu, J. C. Knowles, I. Roy, *Acta Biomater.* **2018**, *71*, 225.
- [48] S. Khan, G. Newaz, *J. Biomed. Mater. Res., Part A* **2010**, *93A*, 1209.
- [49] H. Jahani, F. A. Jalilian, C.-Y. Wu, S. Kaviani, M. Soleimani, N. Abbasi, K.-L. Ou, H. Hosseinkhani, *J. Biomed. Mater. Res., Part A* **2015**, *103*, 1875.
- [50] Z. Li, W. Wang, K. Kratz, J. Kuchler, X. Xu, J. Zou, Z. Deng, X. Sun, M. Gossen, N. Ma, A. Lendlein, *Clin. Hemorheol. Microcirc.* **2016**, *64*, 355.
- [51] L. R. Lizarraga-Valderrama, R. Nigmatullin, B. Ladino, C. S. Taylor, A. R. Boccaccini, J. C. Knowles, F. Claeysens, J. W. Haycock, I. Roy, *Biomed. Mater.* **2020**, *15*, 045024.
- [52] C. Kayal, E. Moeendarbary, R. J. Shipley, J. B. Phillips, *Adv. Healthcare Mater.* **2019**, *9*, 1901036.
- [53] J. B. Leach, X. Q. Brown, J. G. Jacot, P. A. Dimilla, J. Y. Wong, *J. Neural Eng.* **2007**, *4*, 26.
- [54] Y.-C. Huang, C.-C. Huang, Y.-Y. Huang, K.-S. Chen, *J. Biomed. Mater. Res., Part A* **2007**, *82A*, 842.
- [55] M. P. Prabhakaran, J. Venugopal, C. K. Chan, S. Ramakrishna, *Nanotechnology* **2008**, *19*, 455102.
- [56] G. Rosso, I. Liashkovich, P. Young, D. Röhr, V. Shahin, *Nanomedicine* **2017**, *13*, 493.
- [57] J. Tannenbaum, B. T. Bennett, *J. Am. Assoc. Lab. Anim. Sci.* **2015**, *54*, 120.
- [58] C. A. Schneider, W. S. Rasband, K. W. Eliceiri, *Nat. Methods* **2012**, *9*, 671.
- [59] J. M. Curran, S. Fawcett, L. Hamilton, N. P. Rhodes, C. V. Rahman, M. Alexander, K. Shakesheff, J. A. Hunt, *Biomaterials* **2013**, *34*, 9352.
- [60] R. Kaewkhaw, A. M. Scutt, J. W. Haycock, *Nat. Protoc.* **2012**, *7*, 1996.
- [61] M. J. Humphries, *Curr. Protoc. Cell Biol.* **1998**, *00*, 9.1.1.
- [62] W. Sun, C. S. Taylor, Y. Zhang, D. A. Gregory, M. A. Tomeh, J. W. Haycock, P. J. Smith, F. Wang, Q. Xia, X. Zhao, *J. Colloid Interface Sci.* **2021**, *603*, 380.
- [63] M. Usaj, D. Torkar, M. Kanduser, D. Miklavcic, *J. Microsc.* **2010**, *241*, 303.
- [64] J. Popko, A. Fernandes, D. Brites, L. M. Lanier, *J. Int. Soc. Anal. Cytol.* **2009**, *75A*, 371.
- [65] R. Kaewkhaw, A. M. Scutt, J. W. Haycock, *Glia* **2011**, *59*, 734.